# EXPERIMENTAL CHARACTERIZATION OF LASER BASED ULTRASONIC SYSTEM

By

GOLLA DALIRAJU



DEPARTMENT OF MECHANICAL ENGINEERING

Indian Institute of Technology Kanpur

FEBRUARY, 2002

# EXPERIMENTAL CHARACTERIZATION OF LASER BASED ULTRASONIC SYSTEM

A Thesis Submitted

in Partial Fulfillment of the Requirements

for the Degree of

**MASTER OF TECHNOLOGY**

*by*

**GOLLA DALIRAJU**

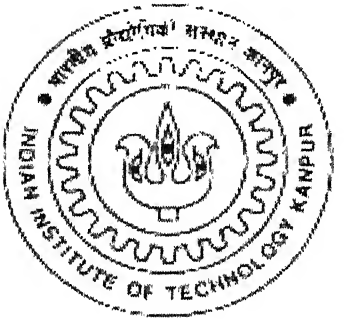


to the

DEPARTMENT OF MECHANICAL ENGINEERING

INDIAN INSTITUTE OF TECHNOLOGY, KANPUR

FEBRUARY, 2002

# CERTIFICATE

20-2-02

It is certified that the work contained in the thesis entitled **EXPERIMENTAL CHARACTERIZATION OF LASER BASED ULTRASONIC SYSTEM** by GOLLA DALIRAJU has been carried out under our supervision and that this work has not been submitted elsewhere for a degree.


Dr.V.Raghuram
(Sr.Research Engineer)
Department of Mechanical Engg.
Indian Institute of Technology, Kanpur.

Dr. N. N. Kishore
(Professor & Head)
Department of Mechanical Engg.
Indian Institute of Technology, Kanpur.

*Dedicated to*

# MY PARENTS

*Who sacrificed their dreams*

*so that mine could come true*

# ACKNOWLEDGEMENTS

I wish to express my gratitude towards my thesis supervisors Dr. N.N. Kishore and Dr.V.Raghuram for their guidance, invaluable suggestions and constant encouragement.

I wish to express my special thanks to Dr. Atul Kumar Agrawal and Mr. S. K. Rathore for their invaluable suggestions and constant encouragement towards completion of my work.

I appreciate and extend my thanks to my lab mates Sqn.Ldr.Sarin, Sajay Kumar Sahoo and Pradipta who worked with me as a team, to ensure the timely commissioning and calibration of the setup. I extend my thanks to my other labmates, Nitesh, Shashi bhushan and Samuel for their co-operation.

I would like to thank Mr. Anirbhan Mitra (Physics Dept.), who helped in the power unit calibration.

I am very much thankful to Shri Trivedi who prepared all test specimens and experimental fixtures in a very short time and professionally. I would be failing in my duty if I do not thank Dr P. Munshi, Dr Prashant Kumar and Dr.K.Muralidhar who spared their valuable time to ensure procurement of Scanning equipment and Fixtures.

I would like to thank all my friends for making my stay at IITK very enjoyable and memorable. I will cherish the moments forever.

Indian Institute of Technology, Kanpur. Golla Daliraju

February, 2002

# ABSTRACT

Non Destructive Evaluation (NDE), in particular ultrasonic technique, is one of the most promising techniques both due to cost effectiveness and high reliability. Although piezoelectric transducers are commonly used for nondestructive testing, several problems are associated with the requirement that they be in contact with the test material with an acoustical impedance matching coupling medium. Laser Based Ultrasonics (LBU) overcome all these problems and affords some interesting applications like non-contact ultrasonic measurements in both electrically conducting and non-conducting materials, in materials at elevated temperatures, in corrosive and other hostile environments, in geometrically difficult locations to reach and to do all of these relatively at large distances, i.e. meters, from the test object surface. The present work involves the development of Nd: YAG Laser Based Ultrasonic system application in the field of Non-Destructive Testing (NDT). The 7mm beam has been characterized. Also studied is the ultrasonic wave generated by the Nd: YAG laser beam on materials like Aluminium, glass-epoxy composites. The detection has also been done using a Laser Based System (He-Ne laser based heterodyne probe). For all the cases, the power distribution within the beam is found to be Gaussian in nature.

***Key words***: power distribution; LBU; beam characterization.

# CONTENTS

## List of Figures

# List Of Symbols

| | |
|---|---|
| $\Omega_S$ | The sampling frequency |
| $f(t)$ | Time-domain Signal |
| $t$ | Time |
| $\tau$ | Time-shift |
| $\omega$ | Frequency |
| $F(\omega)$ | Signal in frequency-domain |
| $w(t-\tau)$ | Window function |
| $a$ | Scaling parameter |
| $b$ | Translation parameter |
| $F(\omega)$ | Fourier Transform |
| $W_f(a,b)$ | Wavelet Transform |
| $\psi(t)$ | Mother wavelet function |
| $C(a,b)$ | Wavelet coefficient |
| $s(t)$ | Ultrasonic signal |
| $y(t)$ | De-noised signal |
| $n(t)$ | Noise |

# *Chapter 1*

# INTRODUCTION

## 1.1 INTRODUCTION

Non-Destructive testing (NDT) plays a vital role in quality assurance of structural members during manufacturing stage and operating life. Ultrasonic testing is one of the most promising techniques both due to its effectiveness and simplicity of setup. Ultrasonic Inspection involves impinging a low energy, high frequency stress pulse into the material under inspection and examining the subsequent propagation of this energy. Defects such as cracks and inclusions act as sources of wave scattering through reflection, refraction, diffraction and mode conversion. Being one of the most commonly used Non Destructive Testing (NDT) methods, Ultrasonic Testing (UT) is developing rapidly in recent years. In this, a piezo-electric transducer (probe) generates ultrasonic waves, which propagate in the elastic medium and are detected either by the same (Pulse echo) or by a different transducer (Through transmission).

Although piezoelectric transducers are commonly used for nondestructive testing, several problems are associated with the requirement that they be in contact with the test material with an acoustical impedance matching coupling medium. For velocity measurements, which are necessary for material thickness measurements and to locate the depth of defects, the coupling medium can cause transit time errors. Due to partial transmission and partial reflection of the ultrasonic energy in the couplant layer, there may be a change of shape of the waveform, which can further affect accuracy of the velocity measurement. This can also lead to serious errors in absolute attenuation measurements, which is the reason that so few reliable absolute measurements of attenuation are reported in the scientific literature. Therefore, a method of non-contact generation and detection of ultrasound is of great practical importance. Several such techniques are presently available in various stages of development, namely capacitive pick-ups, electromagnetic acoustic transducers (EMATs), laser beam optical generators

and detectors, and more recently air (gas)-coupled ultrasonic systems. However, as the name implies, capacitive pick-ups cannot be used as ultrasonic generators and, even when used as detectors, the air gap required between the pick-up and test structure surface is extremely small, which in essence causes the device to be very nearly a contact one. One major problem with EMATs is that the efficiency of ultrasound generation and detection rapidly decreases with lift-off distance between the EMATs face and the surface of the test object. They can obviously be used only for examination of electrically conducting materials. Because of the physical processes involved they are much better detectors than generators of ultrasound. Laser based ultrasound (LBU) generation and detection overcomes all of these problems and affords the opportunity to make truly non-contact ultrasonic measurements in both electrically conducting and non-conducting materials, in materials at elevated temperatures, in corrosive and other hostile environments, in geometrically difficult to reach locations, and do all of this at relatively large distances, i.e. meters, from the test object surface. Furthermore, lasers are able to produce simultaneously shear and longitudinal bulk wave modes as well as Rayleigh and plate modes. These systems have been used to inspect aircraft structures, art paintings, lumber, composite pre-pregs, and composite panels. LBU uses a pulsed laser to generate the ultrasound and a continuous wave (CW) laser interferometer to detect the ultrasound at the point of detection to perform ultrasonic inspection.

By considering the importance of LBU, it is clear that there is a need to characterize the Nd: YAG laser beam, which is used for the same. Characterization of the beam is nothing but the study of the entire beam for each and every input power settings. Better characterization of the beam leads to proper application.

## 1.2 LITERATURE SURVEY

Looking at the history of the lasers, the first laser was invented by Maiman in May 1960. It was a solid ruby laser. First Uranium Laser by IBM labs in Nov., 1960, first He-Ne laser by Bell Laboratories in 1961, first semiconductor laser by Robert Hall at General Electric labs in 1962 and first working Nd:YAG laser and $CO_2$ by Bell Laboratories in

1964[1]. For the power distribution of the He-Ne laser an experiment called knife-edge method is given by Sirohi in his book [2]. Keicher et al [3] performed the experiments on CW Nd:YAG laser to understand multimode laser beam propagation characteristics for better development of laser material processing applications. Scruby and Drain [4] in their introductory book on this subject have elaborated on the principles underlying generation and reception processes of all techniques used. Monchalin [5] has given an elaborate review on discussion of different techniques with reference to exploitation of the power of the laser ultrasonic generation. The review covers knife-edge techniques, optical heterodyning, differential interferometry, and velocity (time-delay) interferometry methods. Huber and Green [6] in their publication have elaborated on the design of a portable fiber-optic heterodyne interferometer for detection of out-of-plane motion on the surfaces. They had successfully coupled this detection system with a compact Nd: YAG laser for generation of ultrasonic waves. Corbel et al [7] showed that a pulsed laser can be used to generate simultaneously elastic waves of different types in laminate composite materials. Castegnede et al [8] reviewed some advances dealing with the charachterisation of composite materials by using laser based ultrasound techniques. They discussed laser interferometer detection and the determination of the theoretical displacement fields. Cho et al [9] carried out an evaluation of subsurface lateral defects, using SAW (Surface Acoustic Waves) generated by a Q-switched YAG laser and monitored by a heterodyne laser interferometer. This fundamental work was carried out on thin metallic foil, the material's properties of bonded layer can be estimated by the velocity dispersion of the Rayleigh wave, and the bond Quality can be estimated by an analysis of the generalised lamb wave. Rathore et al [10] have employed LBU and ray acoustics for establishing a criterion to identify the ray tangential to the defect boundary and evolve a method of reconstruction of the defect to estimate the size and location of the defect. Legendre et al [11] have proposed a wavelet-based method to perform the analysis of NDE ultrasonic signals received during the inspection of reinforced composite materials. By combining the time domain and the classical Fourier analysis, the wavelet transform provides simultaneous spectral representation and temporal order of the signal decomposition components.

This study is carried out on the basis of photographic technique or scanning technique to know the power distribution within the beam given by Sirohi [2]. The photographic technique involves the measurement of the power past a knife-edge, which is slowly inserted in the beam. The scanning technique involves the characterization of the system by interferometry, which leads to better application of the system for non-destructive testing and evaluation.

## 1.3 PRESENT WORK

The present work involves the characterization of the Nd: YAG laser in its use for ultrasonic NDT. In the present work, an experimental setup has been developed using a Nd: YAG pulsed laser for generation of ultrasonic waves in specimens and a He-Ne continuous laser based heterodyne optical interferometric probe for detection of the same. The experimentation includes calibration of the laser setup, and interfacing of the manual scan setup for scanning both homogeneous (aluminium) and non-homogeneous (composites) specimens.

The various portions of the beam at various powers are analyzed. For investigation of the beam characteristics both time and frequency domain features have been analysed. Frequency domain features viz., amplitudes at different frequencies were obtained after performing FFT on the digitized time domain signal. For the energy responses of the different portions of the beam, the average power of each signal received at other side of the specimen is calculated by using Parseval's relation.

Chapter 2 discusses, the various aspects of laser excited ultrasonic technique (LBU).

In Chapter 3, the details of the experimental setup and data acquisition procedure are discussed.

Chapter 4, deals with the FFT, the wavelet analysis and signal analysis techniques.

Chapter 5 presents the results and discussion, with different materials at different input power settings.

Chapter 6, covers the conclusions of the present work and suggestions for the future work.

# *Chapter 2*

# BASICS OF LASER ULTRASONICS

## 2.1 INTRODUCTION

Laser is the acronym of Light Amplification by Stimulated Emission of Radiation. Laser is light of special properties, light is the electromagnetic (EM) wave in visible range. Lasers, broadly speaking, are devices that generate or amplify light, just as transistors generate and amplify electronic signals at audio, radio or microwave frequencies. Here light must be understood broadly, since lasers have covered radiation at wavelengths ranging from infrared range to ultraviolet and even soft x-ray range. The term ultrasonics (above sonic) is used to describe mechanical wave propagated in gases, liquids or solids at frequencies above the upper limit of human hearing i.e. 20KHz and up to 400MHz. Because the characteristics of these waves are influenced by the mechanical properties of any medium through which they pass, one can use ultrasonics to investigate the properties of that medium.

So the laser based ultrasonics is the name given to the techniques in which laser beam interaction with the surface of the test sample is substituted for piezoelectric transducers for launching and probing elastic waves. Since they do not require any mechanical contact, these techniques are very attractive. For example, in the field of NDT, the association of laser generation with optical detection provides a completely remote ultrasonic system. Other fields of applications are: material evaluation, acoustic emission, acoustic emission, photothermal microscopy and acoustic field imaging. According to the intensity of the laser the impact generation method may be classed in two main categories: thermoelastic regime and ablation régime. In the field of NDT surface damage is avoided by means of specific techniques. In concrete testing the structure can tolerate some surface imperfection. There are different methods applied; for example, one uses shock waves, which are generated by laser impact on the sample and optical detection (interferometrics or noninterferometrics), which monitors the induced surface. Other methods are used incorporating contact ultrasonic probes working as

receivers or transmitters. Hence, this method needs no contact medium and the source can be some meters away; it is used especially for applications such as NDT for hot materials.

## 2.2 PROPERTIES OF LASER BEAMS

Laser is characterized by a number of key optical properties, most of which play an important role in the generation of ultrasonic waves. Their four major optical properties are:

(1) Monochromaticity
(2) Coherence
(3) Directionality
(4) Intensity or Brightness

### 2.2.1 Monochromaticity

Monochromatic means the same frequency. Monochromaticity of a laser is reduced by multimode operation of a laser. A small He-Ne laser generally has 3-4 longitudinal modes excited with a spacing of a few hundred MHz, depending on the cavity length. This still gives a bandwidth of a few parts in $10^{6}$. Solid-state lasers tend to have rather large frequency spreads. Monochromaticity is important for some ultrasonic applications, in particular the interferometric measurement of ultrasonic fields.

### 2.2.2 Coherence

Coherence means; is the same order or as a copy of the other photon and in phase with the other photon. Coherence is an important property when it comes to building an optical system to detect ultrasonic waves. In simple words coherence is used to describe how well a wave disturbance at one point in space or time correlates with the disturbance at another point. If there is a well defined phase relationship between the light at two different points in space (i.e. two light beams), or at two different times (i.e. one beam split into two with a delay between the parts, as is typical in an interferometer) than the two light disturbances can be brought together to produce a predictable interference

pattern. If the light is completely incoherent so that there is no predictable relationship (i.e. random phase) between the two disturbances, no interference fringes will be formed. The Fig.2.1 shows the comparison between the ordinary light and laser.

Most techniques involve some form of interferometer, in which good coherence between the reflected and reference beam is essential. Coherence length is the distance of the origin of the beam to the farthest point at which the wave disturbance can be effectively correlated with the disturbance at its starting point. Conventional monochromatic light cannot be used because their coherence length is only of the order of millimeters. The use of a gas laser however enables use of a longer probe than reference beam. This means that a compact instrument (incorporating all except the probe beam) can be built, and that the distance to the sample is not critical.

### 2.2.3 Directionality

Laser beam is highly directional which implies laser light is of very small divergence because of the parallelism of the beam. The radiation produced by a laser is confined to a narrow cone of angles. The beam divergence for a typical gas laser is of the order of 1 milliradian. Commercial He-Ne lasers having divergence of a few tenths of a milliradian are also available. The diameter of the beam is typically about 1mm for a gas laser such as helium-neon, and in the range 1-20mm for a pulsed solid-state laser. The light from gas and solid state lasers thus forms a highly collimated beam which is extremely valuable for laser ultrasonics since it enables the beam to be focused to a very small spot. This means not only high spatial resolution, but also, in the case of ultrasonic displacement measurement by interferometer, the ability to collect a larger fraction of the scattered light from a rough surface, thereby increasing the sensitivity. For laser generation it means that very high incident power densities are attainable. Low beam divergence also means that the beam can travel distances of the order of several meters from the laser to the specimen without appreciable spreading and losses. Thus both laser generation and reception of ultrasound can be made genuinely remote techniques.

### 2.2.4 Intensity or Brightness

Intensity or brightness of a light source is defined as the power emitted per unit area per unit solid angle. A laser beam extremely intense, more intense than any other light source. This is the property for which lasers are best known outside the field of optics. Although the optical power output from a small helium-neon (He-Ne) laser may be only say 2mW, a beam diameter of 0.5mm leads to a power density of about 1 $Wcm^{-2}$. Such a beam can be readily focused by a simple lens to a spot of diameter 0.05 mm because it is monochromatic and coherent. The incident power intensity is then 100 $Wcm^{-2}$.

Intensity is a very important property for laser reception of ultrasound, as sensitivity of a single mode laser interferometer system (defined as signal to noise ratio for a fixed bandwidth) increases with the square root of light intensity, provided other conditions remain constant. The limiting factor becomes the intensity at which the specimen is damaged or otherwise adversely affected by intense irradiation. Increase in power also brings penalties like increase in noise and multimode interference. Intensity is also a crucial factor in the generation of ultrasound by laser since incident power intensities typically in the range of $10^4$-$10^6$ $Wcm^{-2}$ are needed to act as a thermoelastic source of ultrasound.

## 2.3 BASIC PRINCIPLE OF LASER OPERATION

The laser is a device, which amplifies the intensity of light by means of a quantum process known as stimulated emission. Indeed the name LASER is an acronym standing for Light Amplification by Stimulated Emission of Radiation. In what follows, some details are presented for the sake of continuity. The operation of the simplest laser can be readily understood in terms of a quantum mechanical model having say three energy levels $E_0$, $E_1$, $E_2$, such that $E_2>E_1>E_0$. In reality, there may be more than three levels. The ground state is well populated, whereas the intermediate and upper states are sparsely populated. Now an atom absorbs energy in terms of quantum theory and is excited into the upper state, the radiation having a frequency $\nu_p$ such that

$$h\nu_p=E_2-E_0$$

Where h is the Planck's constant. In laser terminology this process is called 'pumping', so that $\nu_p$ is the 'pumping frequency'. Pumping tends to equalize the population of two states so that $E_2$ becomes well populated. Emission can now occur in response to incident radiation, at a frequency $\nu$ given by

$$\mathbf{h\,\nu = E_2 - E_1.}$$

Note that necessarily $\nu \leq \nu_p$, so that the pumping frequency must always be equal to or higher than that of the radiation to be amplified. In order to obtain light of sufficient intensity for practical use, there has to be some mechanism for feeding the energy back into the laser system and thereby building up the amplitude of oscillations in a resonant system. The usual way of obtaining sustained oscillations is to site a high performance mirror at each end of the lasing medium. In the simplest system both mirrors are plane, and accurately aligned perpendicular to the axis of the laser. Thus the light is reflected backwards and forwards through the lasing medium. On each pass it stimulates further emission from the medium and is thus amplified in intensity.

## 2.4 LASERS FOR ULTRASONIC GENERATION

The simple laser arrangement will operate in a pulsed mode if it is pumped for example by a pulsed flash tube. Depending on the type of laser, pulses of duration typically 100 μs to 1ms can be obtained. Although high-energy pulses can be produced in this way, the normal mode is not particularly useful for laser ultrasonics because the pulse duration is too large. An additional technique, known as Q- switching or Q-spoiling, is needed to obtain pulses in the required 1-100ns range. The Q (quality) factor of a cavity resonator is the energy stored in the cavity divided by the energy lost from the cavity per round trip of the light within the cavity. Thus if Q is low the cavity oscillations are suppressed and the stored energy builds up within the lasing medium. When the Q is high, the cavity can support oscillations into which energy is supplied from the medium. Thus switching from low to high Q results in the rapid extraction of power from the laser cavity. Practical Q-

switches are in the form of elements with variable absorption that are inserted between the mirrors. Two commonly used Q switches are the Pockels cell and bleachable (saturable) dye. Also of potential importance to non-contact ultrasonics are lasers that can be pulsed repetitively. Adequate cooling in pulsed solid-state laser is a problem. Hence gas lasers are preferred. However solid-state lasers can store higher individual pulse energies than gas medium lasers. Conventional ultrasonic inspection often uses palpitation rate as high as 1-10 kHz for signal averaging purposes or for speed.

Laser generation of ultra sound does not impose very stringent conditions on the source laser. All that is required is the ability to deliver a reasonably high pulsed energy density to a small area of the specimen, where the pulse length is in the range of 1-100ns. As already mentioned, wavelength is not critical, nor is monochromaticity and coherence. Most researchers have employed a solid state laser, either ruby or Nd:YAG. The Nd:YAG laser has proved itself to be a versatile system under Q-switched conditions. However, the fundamental wavelength (1064nm) is in the near infrared, which makes alignment more difficult than with the visible laser. The frequency-doubled wavelength of 532 nm is in the visible spectrum while the harmonics of 266nm and 355nm are in the ultraviolet zone.

## 2.5 LASERS FOR INTERFEROMETRY

For applications like interferometry, where wavelength purity and coherence are important, continuous wave lasers are to be designed with special optical components. The main problem is that a simple laser will excite a number of longitudinal and transverse modes. The result is that energy is amplified over a narrow range of frequencies instead of the desired single frequency, giving rise to inter mode beat frequencies, and there is a variable distribution of energy across the beam. The generally preferred transverse mode (usually the lowest order mode with circular symmetry, $TEM_{00}$) can be selected, and higher order modes suppressed, by the use of at least one curved (concave) mirror at the end of the cavity and/or a suitable aperture within the cavity. A multimode laser can be employed to minimize the multi-mode problem of longitudinal wavelengths in interferometry and then a balanced detection system and

adjustment of the path difference between the two arms of the interferometer can be used to minimize the effects of intermode beats if necessary.

The recording of ultrasonic waves by laser is dependent upon all the fundamental properties of the laser: monochromaticity, coherence, directionality and power density. Because of its ready availability and excellent optical characteristics, notably monochromaticity and coherence, the helium-neon laser is mostly used. This system is however somewhat limited with regard to maximum power which controls sensitivity. The argon ion laser delivers higher power and is also inherently more sensitive because of its shorter wavelength. Argon ion lasers are however very noisy. Nd:YAG laser is also suitable for application in laser interferometers.

## 2.6 LASER-GENERATED ULTRASOUND MODES

The use of a pulsed laser to generate broadband acoustic signals is now well established; three basic mechanisms of ultrasonic generation have been identified:

**(I) The thermoelastic regime:** A laser emits a beam of coherent radiation whose wavelength may be in the infrared, visible, or ultraviolet part of electromagnetic spectrum. When this is incident on a solid sample, in general some of energy is absorbed by various mechanisms, depending upon the nature of the sample and the frequency of the radiation, while the remainder is reflected or scattered from the surface. At low incident power densities, electromagnetic radiation from the laser is absorbed in the surface region of a sample, causing localized heating as shown in Fig.2.2. Thermal energy then propagates into the specimen as thermal waves. The heated region undergoes thermal expansion and thermoelastic stresses generate elastic waves (ultrasound), which propagate deep within the sample. For typical Q-switched laser pulse durations a thermal wave filled only extends a few micrometers even in good conductors. Contrast the incidence of low frequency modulated light where the thermal field extends millimeters or centimeters and is itself useful for materials characterization.

**(II) The constrained surface source:** Constrained surfaces include coating the surface with a thin solid layer of, for instance, paint or rust and roughness, covering the surface with a transparent solid such as glass, covering the surface with a transparent liquid, and

finally constraining a thin layer of liquid between a transparent solid and the solid. All these four techniques modifying the surface of the sample introduce large stresses normal to the surface, as shown in Figs.2.3 (a) to 2.3 (d), which are otherwise absent for the thermo elastic source at a free source. The form of the ultrasonic source is thus substantially modified. For different combination of stresses generates a different ultrasonic sound field, with considerable enhancement in compression wave amplitude, especially propagating normal to the surface. The constrained surface source generates a sound field more akin to that of ablation, but at lower power densities and without any damage. However, the need to constrained with to instance a liquid, reduce the usefulness of the laser ultrasonic source for many non-destructive applications.

**(III) The plasma regime:** At high incident power densities, surface melting and evaporation occur, resulting in material ablation and the formation of plasma above the sample surface as shown in Fig.2.4. The momentum of the evaporated material exerts an opposite force on the sample, causing a reactive stress at the surface. This generates an intense broadband ultrasonic source, whose strongest components are, directed normal to the surface. The effects caused by the plasma generated in association with ablation in case of Q-switched lasers are:

- The plasma exerts a high pressure on the surface, which in turn suppresses vaporization of the material by raising boiling point of the material well above its normal value.
- It absorbs light from the laser pulse; acting as a shield, but also becoming extremely hot.
- As it expands it produces an impulse reaction on the surface.
- It radiates some of its heat back on to the surface, maintaining its high temperature for some time after the incident lower pulse power has started to fall.

In this study, vacuum grease was applied to sample surface to enhance the signal, and ultrasound was thus generated by a combination of I, II and III above.

## 2.7 METHODS OF INTERFEROMETRY

Interferometers for the detection of ultrasonic movements of waves may be divided into two main types. In the first type, light scattered or reflected from a surface is made to interfere with a reference beam, thus giving a measure of optical phase and hence instantaneous surface displacement. The second type of interferometer makes use of interference between a large number of reflected beams. This is designed as a high-resolution optical spectrometer to detect changes in the frequency of the scattered or reflected light. It thus gives an output dependent on the velocity of the surface. The first type is the more widely used and the most practical at lower frequencies and with reflecting surfaces. The second type offers a potentially higher sensitivity with rough surfaces at higher frequencies.

For the detection of ultrasonic waves at a surface, the techniques are admittedly insensitive compared with piezoelectric devices. They do, however, offer a number of advantages.

(1) The potential for rapid area scanning, non-contacting (no couplant) generation and no fundamental restriction on surface temperatures.

(2) High spatial resolution may be obtained without reducing sensitivity; the measurements may be localized over a few micrometers if necessary.

(3) As the measurements may be directly related to the wavelength of the light, no other calibration is required.

(4) They can have a flat broadband frequency response, something difficult to achieve with piezoelectric transducers, particularly at high frequencies.

## 2.8 HE-NE LASER HETERODYNE INTERFEROMETER

### 2.8.1 Principle of Detection

The complex amplitude of a laser beam of frequency $f_L$ can be written as:

$$\mathbf{L} = \mathbf{e}^{2i\Pi f_L t}$$

This is divided into a reference beam and a signal beam, whose complex amplitude is:

$$R = r.\, e^{2i\Pi f_L t}$$

The reference beam does not experience any perturbation, however the signal beam experiences a frequency shift $f_B$ in the Bragg cell. Upon reflection on the object, its phase is modulated by the displacement of the sample:

$$\varphi(t) = 4\pi.d(t)/\lambda$$

Where $\lambda$ is the wavelength of the laser beam and d (t) the mechanical displacement of the object. The complex amplitude of the signal beam is therefore:

$$S = s.e^{2i\pi f_L t + 2i\pi f_B t + i\varphi(t)}$$

The interference of the two beams on the photodetector produces an electrical signal at frequency $f_B$, phase modulated by the displacement of the object:

$$I(t) = I_0 + I(t)$$

$$I(t) = k\cos(2\pi f_B t + \varphi(t))$$

The useful signal is contained in the signal delivered by the photodetector as a phase modulation of the carrier frequency. The signal processor delivers an electric signal proportional to the displacement of the object. Half of the current i(t) is filtered at the frequency $f_B$, and phase shifted by 90°. It is then mixed with the other half, non perturbed, and yields a current:

$$j(t) \propto \cos(2\pi f_B t + \varphi(t)) \times \cos(2\pi f_B t + \pi/2)$$

$$j(t) \propto 1/2[\cos(4\pi f_B t + \varphi(t) + \pi/2) + \cos(\varphi(t) + \pi/2)]$$

The signal at the frequency 2 $f_B$ is filtered, to give:

$$s(t) \propto \sin\varphi(t)$$

If the displacement is very small compared to the optical wavelength, this signal can be written as:

$$s(t) = k.4\pi.\, d(t)/\lambda$$

The final electrical signal is therefore directly proportional to the displacement of the object.

### 2.8.2 Working of Heterodyne Interferometer (optics)

The system consists of an optical head. The optical layout is shown in Fig. 2.5. The laser beam emitted by the laser source is horizontally polarized, is directed in the interferometer by two deflecting mirrors. The laser beam is split into two parts by the beamsplitting cube. The reference beam is reflected by the beamsplitting cube and goes through the Dove prism. It is then transmitted by the polarizing beamsplitting cube and deflected by the mirror on the photodetector. The probe beam is transmitted by the beamsplitting cube and is horizontally polarized. Its optical frequency is shifted in the Bragg cell, and transmitted by the polarizing beamsplitting cube. A quarter wave plate transforms the horizontal polarization into circular polarization. The lens focuses the beam on the surface of the sample.

The probe beam is then phase modulated upon reflection on the sample by the mechanical displacement. After the second pass in the quarter wave plate, the direction of polarization becomes vertical. The probe beam is reflected by the polarizing beamsplitter on the photodetector. Just after the polarizing beamsplitter, the polarization of the probe and reference beam are respectively vertical and horizontal. These two beams can therefore not interfere. The analyzer selects a common component at 45° of the two polarizations, thus allowing interference. The photodetector delivers a beat frequency of the Bragg cell phase modulated by the mechanical displacement of the object.

### 2.8.3 Sensitivity

Laser ultrasonics suffers from a lack of sensitivity relative to conventional ultrasonics as the photon structure imposes a fundamental limit on the change in light levels during generation / detection of lasers.

Overall sensitivity to flaws is given by:

$$\textbf{Sensitivity} = T \times f(\sigma, A) \times R$$

Where T, $f(\sigma, A)$, R are terms related to the transmitted sound, the focal or imaging properties of the system determined by the flaw scattering $\sigma$ and the focal aperture A, and the receiver sensitivity. The generated signal can be improved using tailored surface coatings or by increasing the power of the generating source. However this approach is limited by the onset of ablation in the target.

## 2.9 CLOSURE

In this Chapter, the basic theory of generation of ultrasonic waves by lasers and their detection using laser-based interferometers has been presented. Some of the important properties of lasers related to aspects of generation and detection of ultrasonic waves have been discussed. Advantages of using laser based detectors despite poorer detectivity and sensitivity has also been explained.

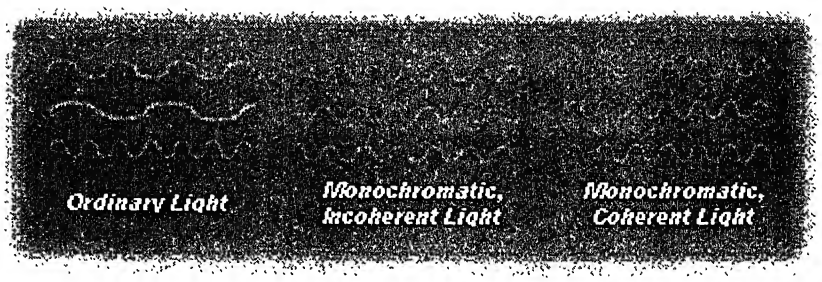


Fig.2.1 Comparison of ordinary light and laser light.

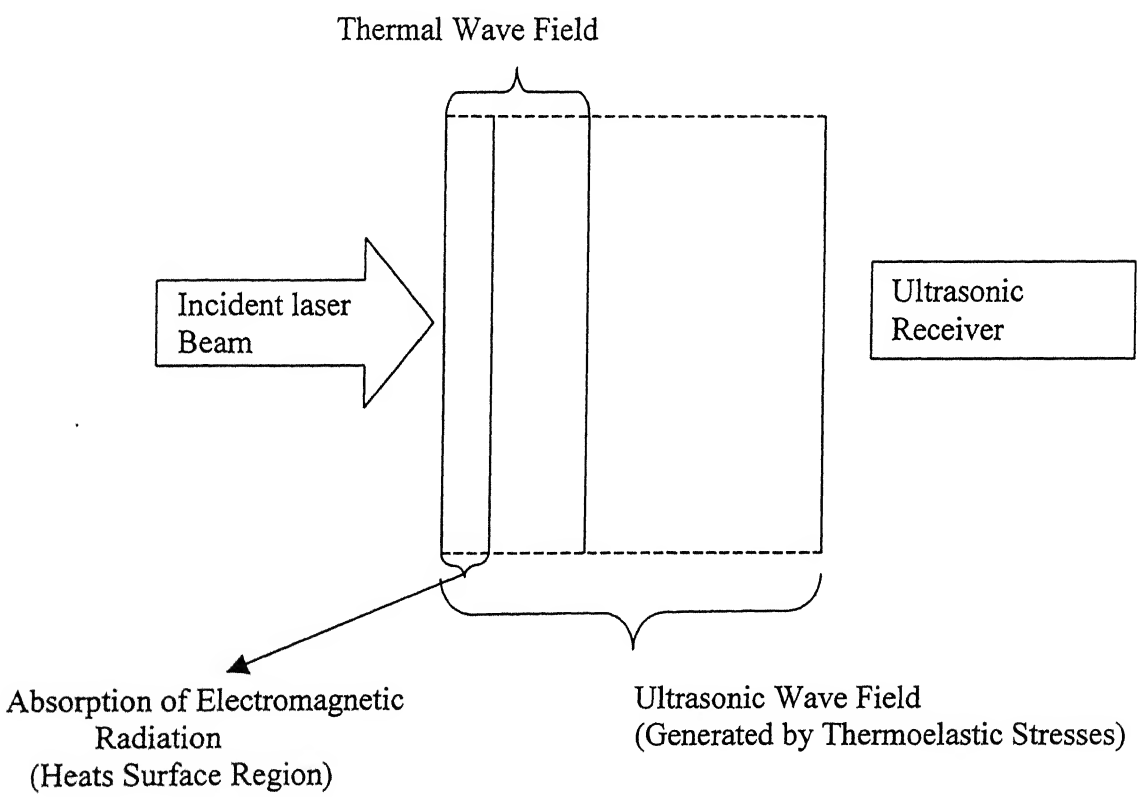


Fig.2.2 Thermoelastic regime

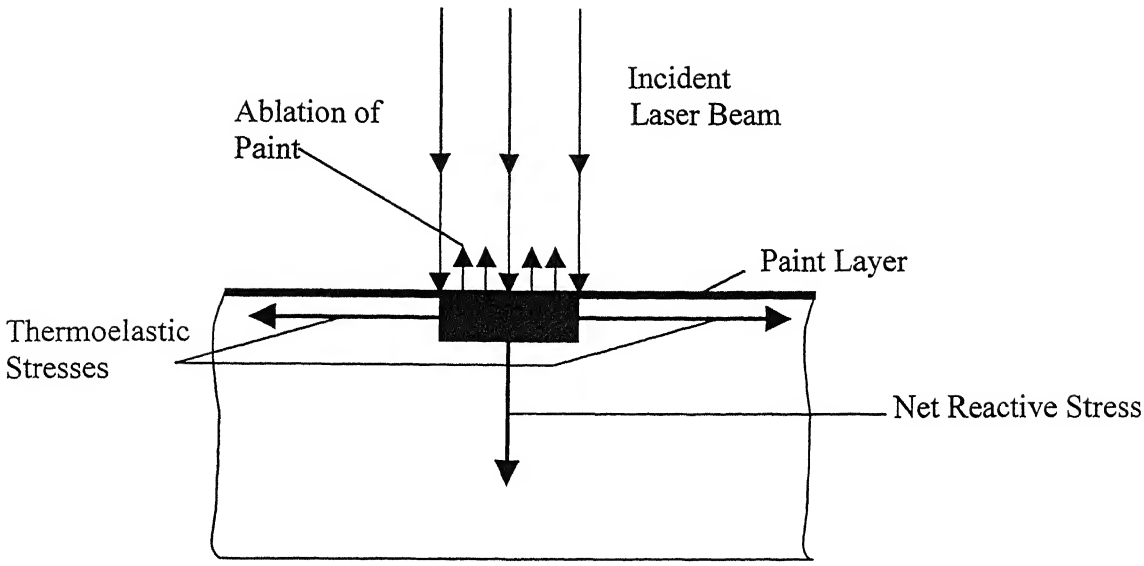


(a) Paint Layer

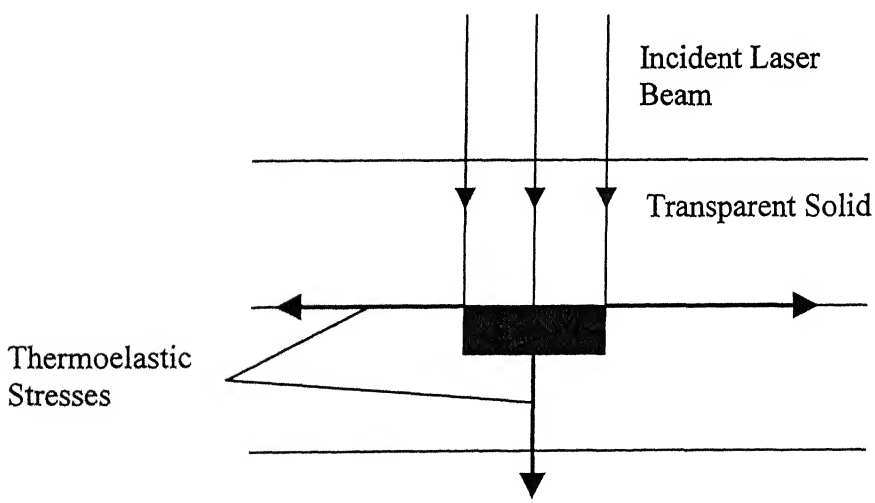


(b) Solid constraining layer

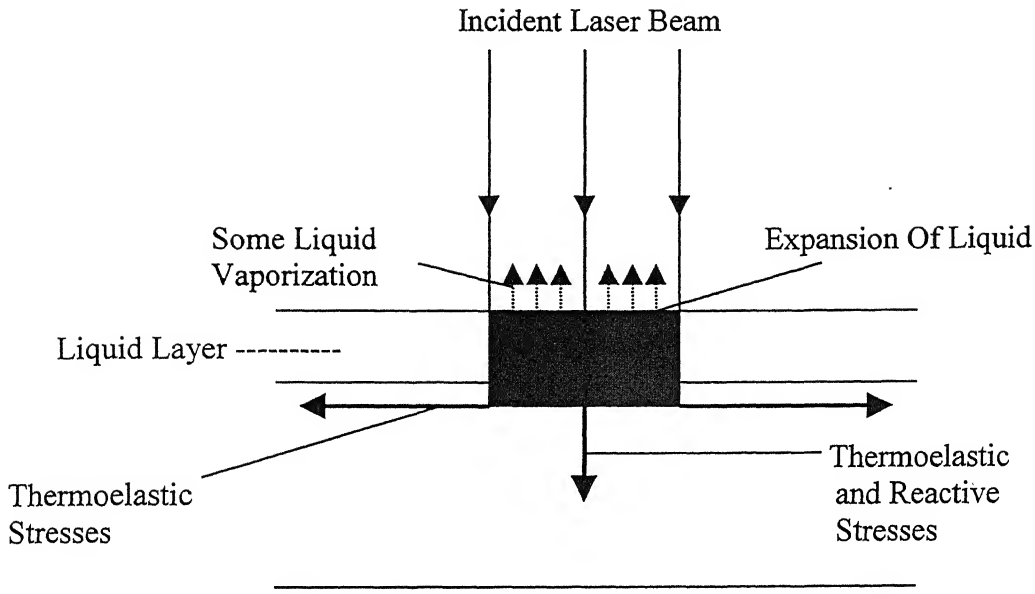


(c) Liquid Layer

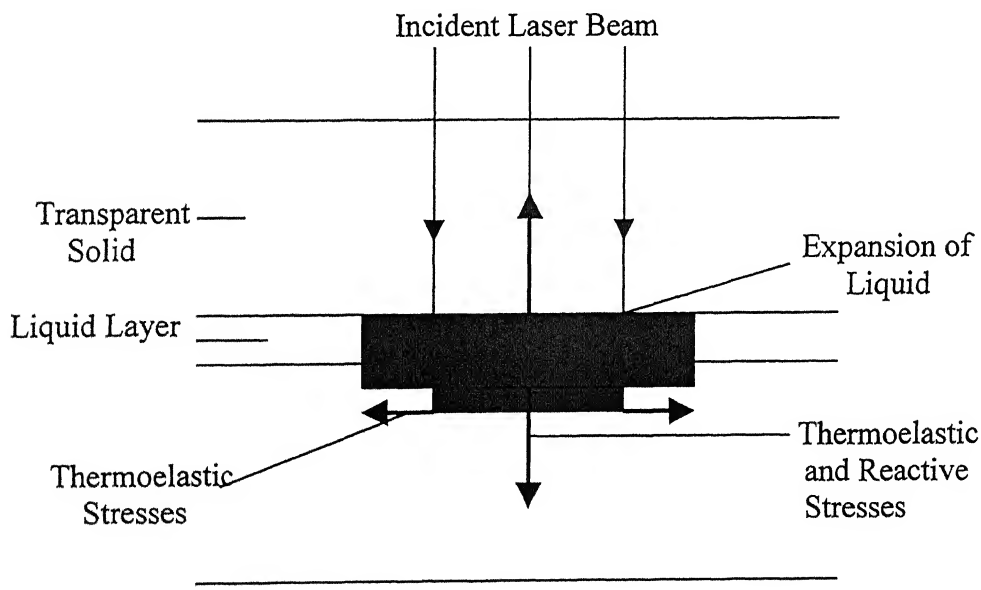


(d) Constrained Liquid Layer

Fig.2.3 Schematic diagram showing stresses induced in a laser pulse incident on a sample surface covered by (a) a thin layer of paint, (b) a thick transparent solid (c) a layer of liquid (d) a layer of liquid constrained by a transparent solid.

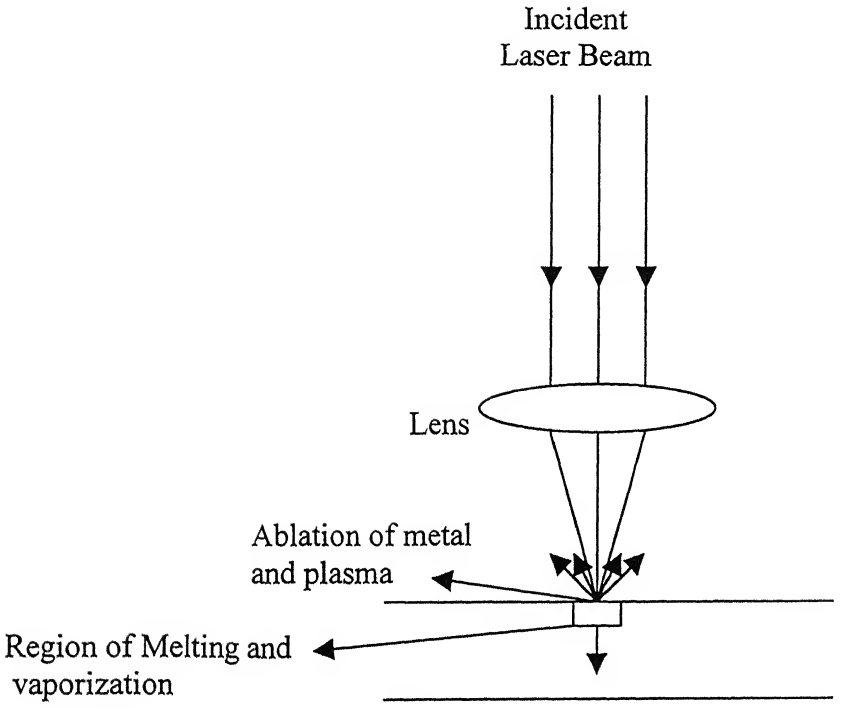


Fig.2.4 Schematic diagram to show ablation of surface material and net reactive force on sample.

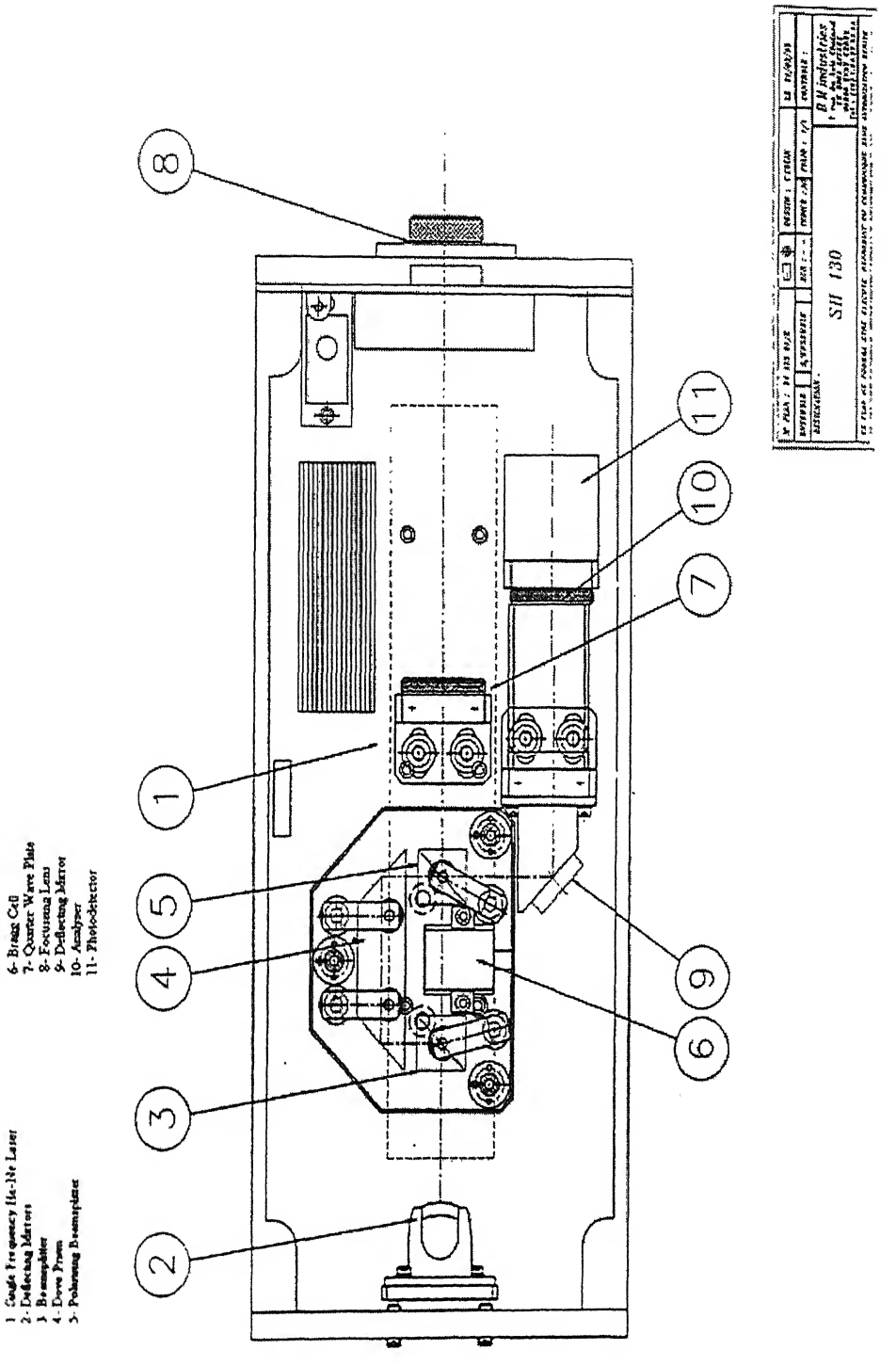


Fig.2.5 Optical Layout of Heterodyne Interferometer

*Chapter 3*

# EXPERIMENTAL SET-UP AND PROCEDURE

This Chapter briefly describes the details of laser based ultrasonic setup and data collection.

## 3.1 EXPERIMENTAL SETUP: LASER BASED ULTRASONICS

Nd: YAG Pulse Laser is used to generate ultrasonic waves in any media, which is to be inspected. Heterodyne type Laser Interferometer is used to detect the transmitted wave, the signals are then amplified and digitized using a Yokogawa DL1740 digital oscilloscope. The oscilloscope is triggered using a synchronization signal from the pockels cell of the pulsed laser. Recorded waveforms are transferred to a HP Pentium III computer over a USB/Ethernet interface for subsequent storage and analysis which is then captured in a Digital Storage Oscilloscope. The schematic layout of experimental setup is shown in Fig.3.1 and a photograph of the same is shown as Fig. 3.2. Small part of the beam is allowed to fall on the specimen to study the Nd: YAG laser beam characterizations. For this purpose the Teflon material with different slits viz. rectangular of 10mm x 1mm, circular slits of $\phi$1mm, $\phi$2mm, $\phi$3mm and circumferential slits of 1mm width at the mean radii at 4mm, 5mm, 6mm were used. All these slits are made in $\phi$25mm Teflon material. A brief description of the setup is given in the following paragraphs.

### 3.1.1 Nd: YAG Pulsed Laser Ultrasonic Generator

The 5000 DNS series pulsed Nd: YAG laser is built on a modular concept. The optical configuration allows variable setting of the optical parameters. It consists of 3 major components, the laser-head, the power supply and the cooling unit. The heart of the system is the pumping structure, which houses the Nd: YAG rod and the flash lamp. The lasers are built on an electro-optically Q-switched oscillator. This oscillator uses a pockels cell Q-switch to produce pulses of high intensity and short duration (5-7 ns). Q- Switched Lasers are often used as a non-contact ultrasound source in non-

destructive testing of materials. Q-switched lasers typically have nanosecond (ns) pulse durations and generate broadband ultrasound waves, though longer laser pulses, of 100 microseconds or greater, have been used for NDE. A variable reflectivity output coupler allows the extraction of high energy on a single spatial transverse mode. This leads to laser beams of low divergence, and to high conversion efficiencies in the harmonic wavelengths (1064, 532, 355, 266 nm). Different harmonic generators extend the wavelength range to the second, third and fourth harmonics.

The active medium of the laser operates on transitions of triply ionized Neodymium atoms ($Nd^{3+}$), which take place of another ion (Yttrium) in the host: Yttrium Aluminum Garnet known by the acronym YAG. The laser operates as a 4-level system. The intense broad-spectrum light of the flash lamp populates the upper level. Once in the higher energy level, the Neodymium ions drop to a metastable level, producing a population inversion. The lower level decays by a fast non-radiative process to the ground state. The strongest Neodymium line is 1064 nm.

### 3.1.2 Optical Heterodyne Laser (He-Ne) Probe

The SH-130 probe is designed to measure transient mechanical displacements of very low amplitude. It is specially devoted to measuring displacements generated by the propagation of an acoustic or ultrasonic wave. The system consists of a compact optical head and an electronic signal-processing unit. The optical head integrates high stability, low power laser source for fast detection with a high spatial resolution.

The electronic signal processor delivers a response proportional to the displacement of the target, with a high bandwidth. The output signal is automatically calibrated to give the absolute value of the measured displacement. The principle of detection (heterodyne interferometry) makes the system insensitive to external vibrations. The compactness of the system allows for a wide range of operating conditions.

### 3.1.3 Digital Storage Oscilloscope (DSO)

The setup utilizes a Yokogawa DL1740 (four channel, one GSa/sec, 500 MHz) Digital Storage Oscilloscope, having built in Zip drive, Ethernet, USB, GPIB and Serial Ports for communication with external PC's/ systems.

### 3.1.4 Computer

The DSO is interfaced to a Pentium III based PC and Data is stored on-line using communication through USB and Ethernet ports.

## 3.2 EXPERIMENTAL PROCEDURE (LBU)

### 3.2.1 Installation And Calibration Of Setup

The calibration of the optical probe involved the following procedural steps:

(1) Mounting of Test Specimen. All tests were carried out on a piezo-electric ceramic specimen prepared with one side having an extremely high reflective surface. The source and receiver are aligned on opposite sides of a parallel-sided sample.

(2) Alignment of the SH-130 Optical Probe. This involved optimizing the control signal by adjusting the orientation of the sample, and fine-adjustment of its distance from the focusing lens. (The focal length of the focusing lens is around 215 mm.)

(3) The photo detector output was measured without going through the signal processor. This was found to be 310 mV (As per specifications). Print out of the DSO image is placed at Appendix 'A'.

(4) The output was then taken through the signal processor with the automatic gain control switched on. The measured signal was found to be in excess of the stipulated signal level of 630 mV peak to peak on 50Ω. (Found to be 730 mV.) This was adjusted using the adjustments available in the signal-processing unit. Print out of the DSO image is placed at Appendix 'B'.

(5) Sensitivity: A sinusoidal voltage, of frequency higher than 200 kHz, (263 kHz) was applied to the sample. The non-demodulated signal was taken into a separate channel of the DSO and spectrum analysis was carried out using Matlab. The demodulated signal was taken to another channel of the DSO. The voltage applied to the sample was adjusted so that the ratio between the carrier at 70 MHz and the sideband at 70 MHz +>200 KHz is 40 dB, which corresponds to a displacement of 10 A° amplitude. The corresponding voltage was measured on the Oscilloscope and the calibration factor was calculated. The accuracy of the measurement was

within the stipulated ten percent limits. The measured sensitivity was 10 mV/ A°. Print out of the DSO image is placed at Appendix 'C'.

(6) Detectivity: To ascertain the detectivity, voltage applied to the sample was decreased until the signal to noise was equal to one. This was visually ascertained on the DSO as laid down in the technical manual. The measured displacement was determined and the detectivity was calculated. The measurement was repeated for each standard bandwidth (4,18 and 45 MHz). The measured detectivity was found to be higher than that recorded at the manufacturers facility, this was primarily due to additional focusing and signal collection arrangements at the input of the optical probe available with them. The detectivity however was found to be within requirements of the existing setup. Print out of the DSO images is placed at Appendix 'D'.

### 3.2.2 Preparation Of Specimen

The present beam characterization is done on both homogeneous (Aluminium) and non-homogeneous (Unidirectional $30^0$,$45^0$,$60^0$ Glass epoxy composites) materials. The dimension of the aluminium specimen is 41mm x 41mm x 4.64 mm and the faces of this specimen was polished to obtain better signal. The Unidirectional Glass epoxy are prepared by hand lay up technique, using roving 600 TEX hot epoxy grade (16plies) manufactured by M/S Nikhil fibers Pvt. Ltd. New Delhi (India). The curing was done at 120° C and 5 Atm pressure for one hour followed by one hour at 150° C and 5 Atm pressure and left to cool to room temperature at same pressure overnight. The dimensions of the finished specimens were 40 x 40$mm^2$.

All the Teflon materials with different slits, as shown in Fig.3.3, were prepared by using conventional machining processes.

### 3.2.3 Scanning Procedure

The specimen is cleaned and center point is marked to get the alignment of Nd: YAG and He-Ne laser. The portion of the specimen facing to He-Ne laser is pasted with retro reflective tape to get the good signal. The scanning procedure with the different slit is as follows.

### 3.2.3.1 Scanning with rectangular slit

A Teflon piece having 10mm x 1mm rectangular slit was fitted on a micrometer controlled device, mounted on the optical test bench. The slit is placed perpendicular to the test bench. The vertical slit was moved horizontally from one end of the beam to the other end in steps of 1mm with the help of the micrometer-controlled device. The mirror, which is shown in the Fig.3.1, was adjusted to point the beam at the center of the specimen for each and every position of the slit. Same procedure was followed for all the specimens viz. aluminium, Unidirectional $30^0$, $45^0$, $60^0$ glass epoxy composite materials. This test was repeated for various input power settings of the Nd: YAG laser.

### 3.2.3.2 Scanning with 1mm hole

The above procedure was followed by using a 1mm hole instead of 10mm x 1mm rectangular slit on the aluminium material.

### 3.2.3.3 Scanning in the radial direction

A Teflon piece having 1mm hole was fitted on a micrometer controlled device, mounted on the optical test bench. Then the center of the hole was made straight with the center of the Nd: YAG laser and the mirror was adjusted to point the beam at the center of the specimen. This test was repeated for various input power settings of the Nd: YAG laser. The same procedure was followed for Teflon pieces having 2mm, 3mm holes and also for Teflon pieces having circumferential slit of 1mm width at mean radii 4mm, 5mm and 6mm as shown in Fig. 3.3.

### 3.2.3.4 Scanning in the ablation mode

The power of the beam was increased to a high level and was focused at the center of the aluminium specimen by using the lens and mirrors as shown in the Fig.3.1. The specimen was scanned at three positions i.e. at focal length, 10mm before focal length and 7.5mm after focal length to study the frequency domain features.

The Nd: YAG laser was pointed onto the specimen using an arrangement of optical mirrors (as shown in Figure 3.1) so that it acts as a source and is perpendicular

to the irradiated surface of the specimen. The scanning is performed at setting corresponding to 1064nm wavelength for the Nd: YAG laser. The He-Ne laser is focused on the opposite side of the specimen at the focal length of the collection lens (approx 215mm). The output of the Optical probe was fed to the electronic signal-processing unit. The electronic signal processor delivers a response proportional to the displacement of the target, with a high bandwidth. The output signal is automatically calibrated to give the absolute value of the measured displacement. This is fed to the oscilloscope where it is displayed and storage of the data is carried out on line in the PC interfaced to the oscilloscope.

## 3.5 CLOSURE

In this Chapter the details of experimental setup and procedure for beam characterization were presented both in the axial direction and radial direction of the beam. Experimental procedure for data acquisition was also explained.

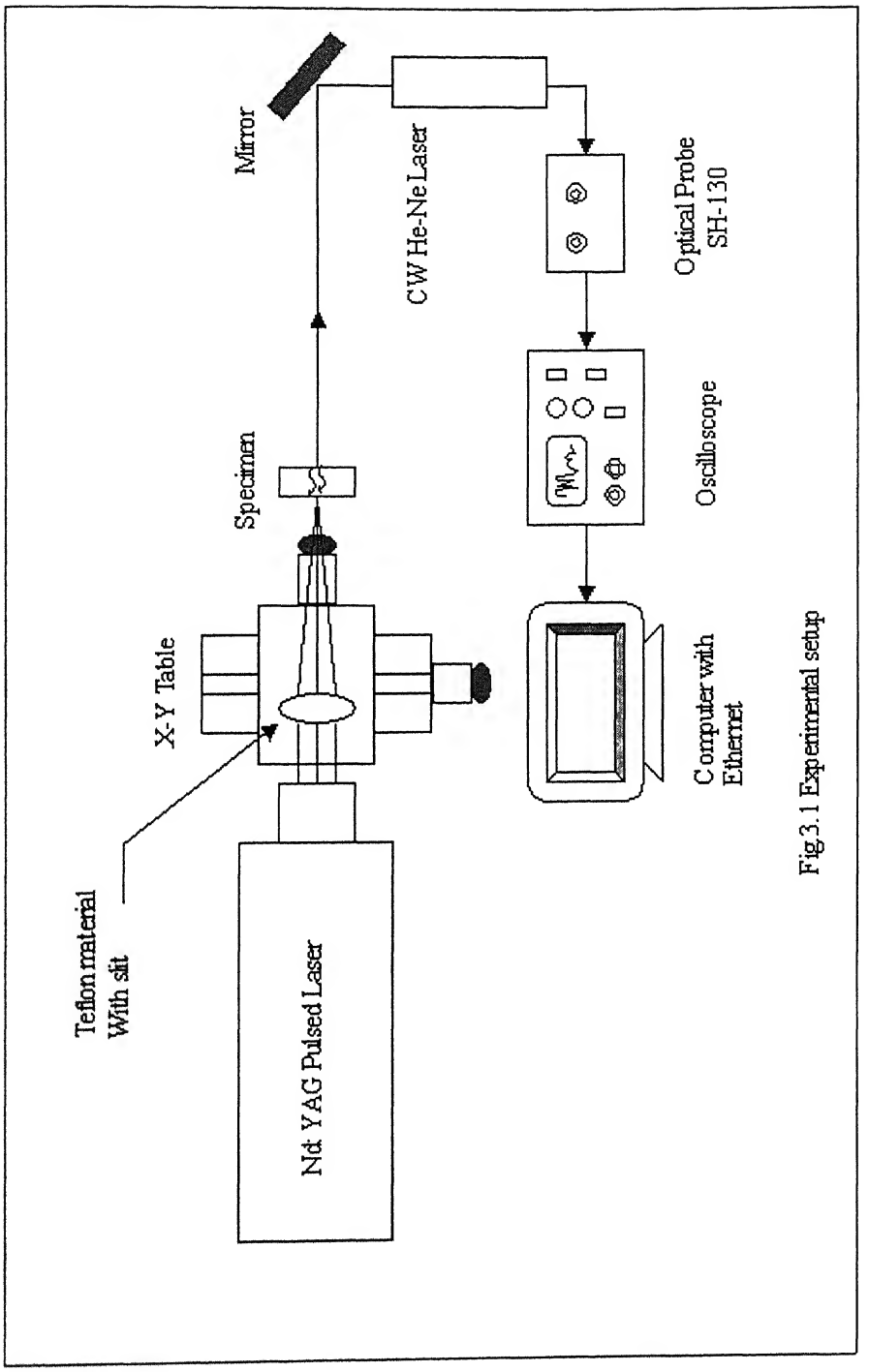


Fig.3.1 Experimental setup

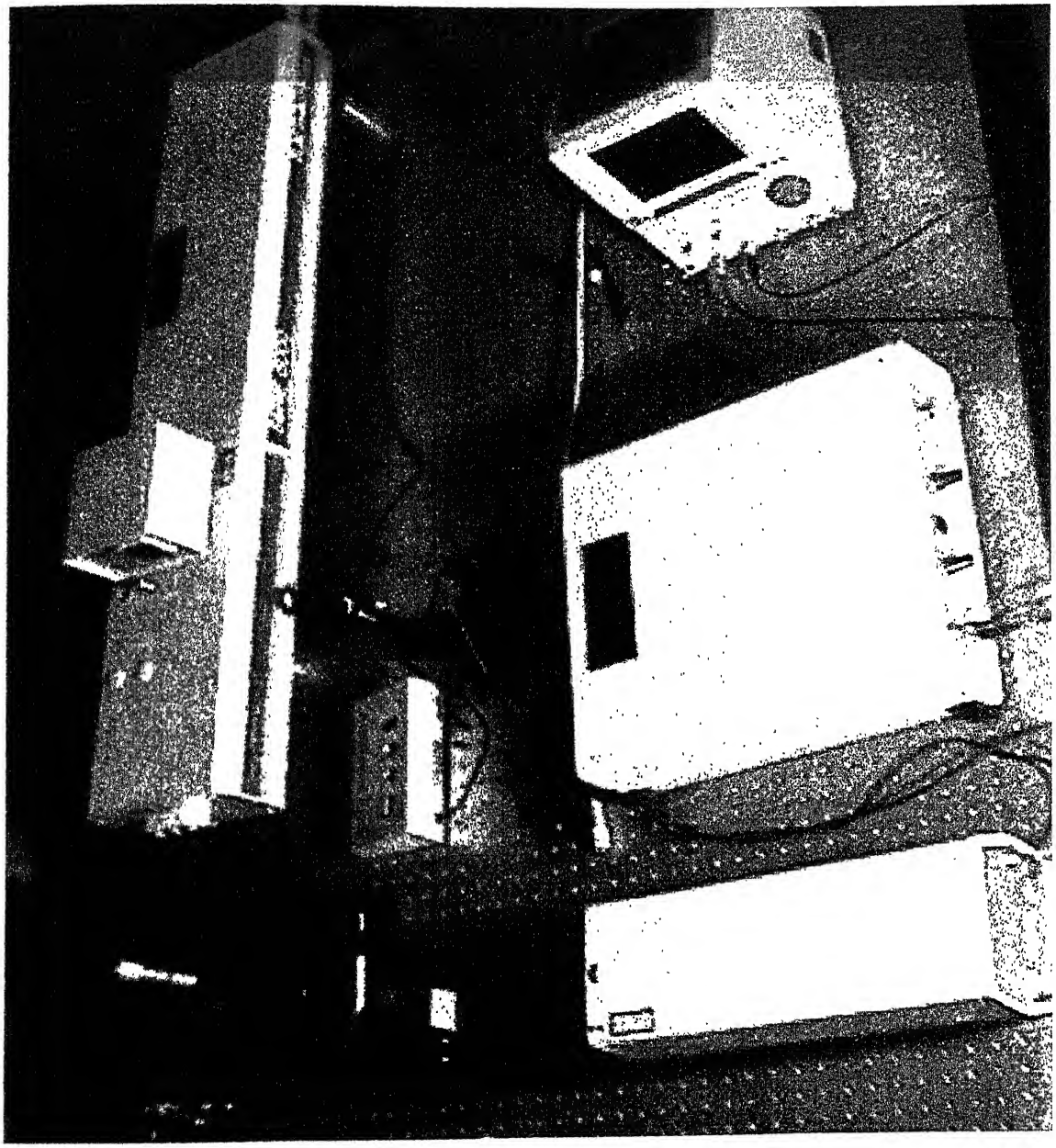

Fig.3.2 (a) Photograph of LBU set-up

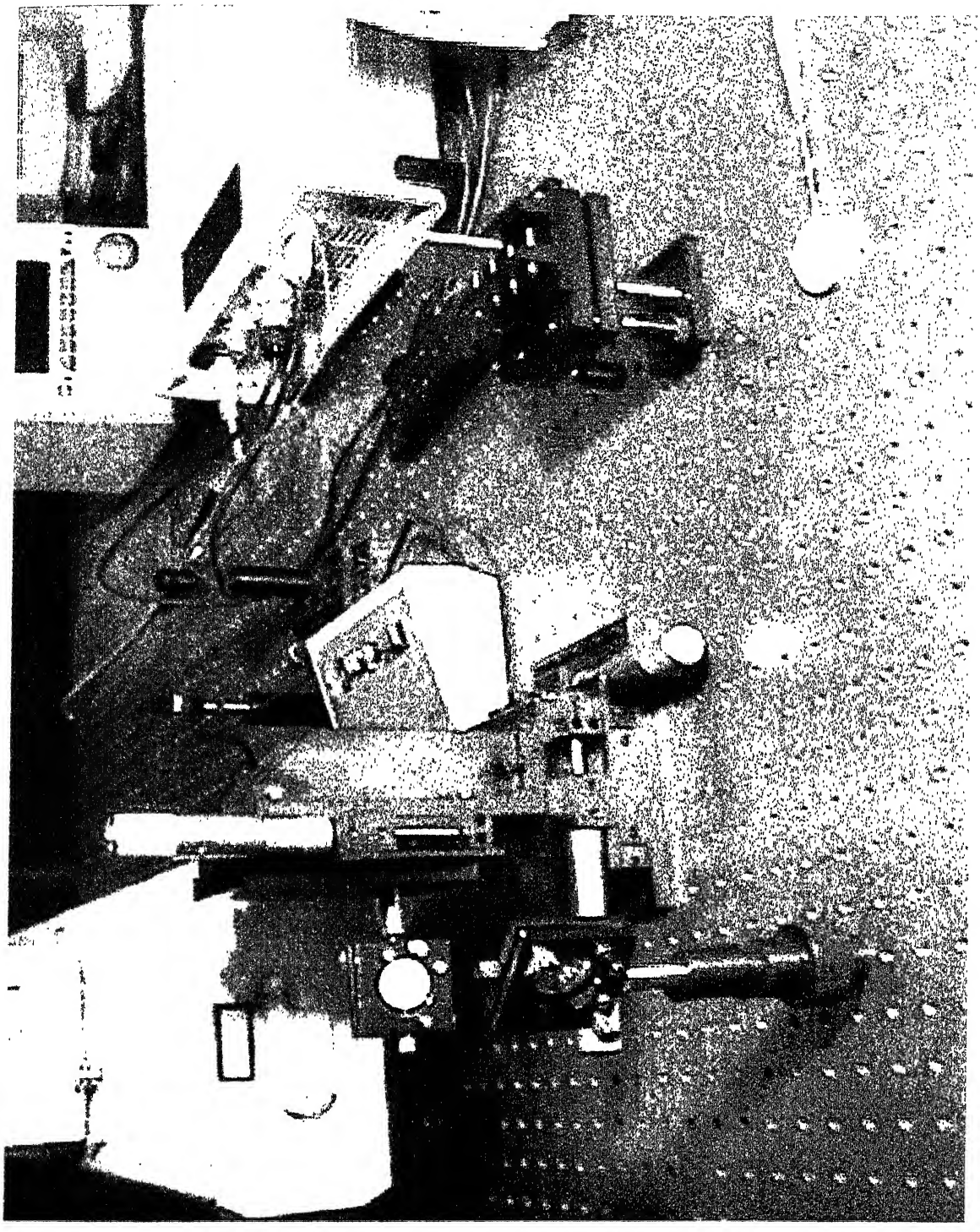

Fig.3.2 (b) Photograph of LBU set-up

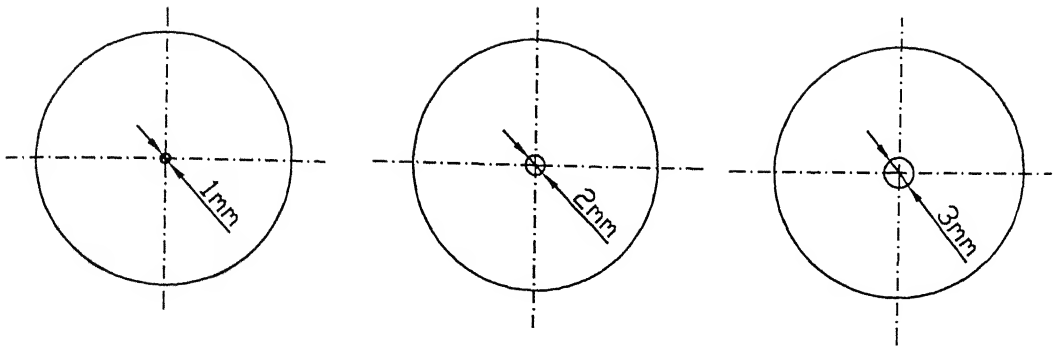


Holes

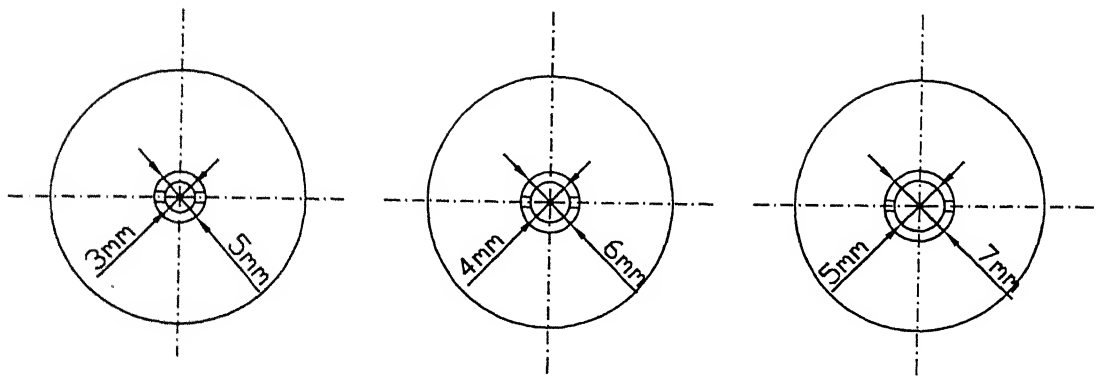


circumferential slits

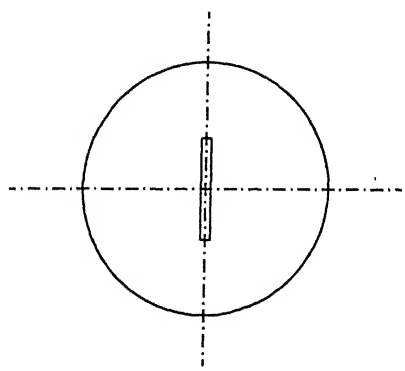

10mm x 1mm
rectangular slit

Fig3.3 Teflon slits

*Chapter 4*

# BASICS OF SIGNAL PROCESSING, WAVELETS AND FAST FOURIER TRASFORM

## 4.1 INTRODUCTION

To characterize the beam type, specific information in the form of features, must be extracted from the digital signal. In relation to ultrasonics, peak amplitude, time of flight, rise time, pulse duration, fall time, may be some of the time domain features and amplitude of different frequency components or harmonics, phase values may be the frequency domain features. In the present study, algorithms developed using Fast Fourier Transform (FFT), to transform the signal from time domain to frequency domain. The transformed signal waveform is also called the amplitude or power spectrum. Then the energy of signal has been calculated from power spectrum of the signal.

In the present work an algorithm has been used based on wavelets transform in order to enhance flaw visibility. Wavelet transforms have generated much interest in various applications such as speech coding, pitch detection, image compression, multiresolution analysis and estimation of multiscale processes. The idea of examining signals at various scales and analyzing them with various resolutions has, in fact, emerged independently in many fields of mathematics, physics and engineering. Wavelet decomposition introduces the notion of scale as an alternative to frequency and maps a signal into a time-scale plane. Each scale in the time-scale plane corresponds to a certain range of frequencies in the time-frequency plane. By combining the time domain and the classical Fourier analysis, the wavelet transform provides simultaneous spectral representation and temporal order of the signal decomposition components.

## 4.2 DIGITAL SIGNAL PROCESSING

Digital Signal Processing (DSP) concepts were introduced many years ago and later emerged as the primary means of detecting, conditioning and automatically classifying a

variety of signal types. Unfortunately Ultrasonic Nondestructive Evaluation (UNDE) and UNDE Instrumentation Development have not exploited the advantages offered by DSP implementations as much as one would expect. This is in spite of the fact that compared to analog signal processing systems; digital systems have the following advantages:

1. Greater Signal Transmission Fidelity
2. Large Non-volatile Storage capabilities
3. Processing/calculation/classification capabilities, and
4. More sophisticated filtering and signal analysis methods

### 4.2.1.Digitizing the Time Axis

A continuous time analog signal $x_a(t)$ has to be converted into a sequence of discrete time signals, represented by a sequence of numbers x, denoted x [n], with n being the $n^{th}$ number in the sequence. Such a sequence is the result of periodic sampling of the continuous time analog signal $x_a(t)$,

$$\mathbf{x[n] = x_a(nT)}$$

T is the sampling period, and 1/T the sampling rate or sampling frequency. For ultrasonic applications this is typically in the MHz range. The sampling frequency, $\omega_S = (1/T)$, has to be greater than the bandwidth $\omega_N$ of the signal being sampled. More precisely, according to the Nyquist Sampling Theorem, for a correct representation of a digitized signal, the sampling frequency $\omega_S$ has to be at least twice as high as the bandwidth $\Omega_N$:

$$\omega_S = 2\pi/T > \omega_N$$

Under-sampling, or sampling at rates less than the Nyquist requirement will cause "aliasing", which results in "shadow frequency images" of the original signal.

### 4.2.2. Digitizing Signal Amplitude

The A/D converter performs the initial amplitude discretization for the input analog ultrasonic signal prior to further conversion needed during processing by either a fixed or floating-point signal processor. This conversion process quantizes the signal amplitudes

into a sequence of finite-precision samples. The precision or quantization error is determined by the number of amplitude quantization levels. This quantization error can be represented as an additional noise signal component.

### 4.2.3. Time and frequency

Fourier analysis is well known technique of signal processing, which breaks down the signal into constituent sinusoids of different frequencies. The *Fourier Transform* (FT) is a technique to transform time-domain signal f(t) into frequency- domain signal F(ω). Fig.4.1 shows an example of the *Fourier Transform*. Mathematically the *Fourier Transform* is given by

$$F(\omega) = \int_{-\infty}^{\infty} f(t).e^{-i\omega t}.dt$$

and its inverse,

$$f(t) = \int_{-\infty}^{\infty} F(\omega).e^{i\omega t}.d\omega$$

where, $\omega$ is the frequency. In *Fourier Transform,* the main drawback is that the time information is hidden. When looking at a FT of a signal, it cannot be seen when the particular spectral components appear exactly in the signal.

### 4.2.4 Short time Fourier analysis (STFA)

*Short-Time Fourier Transform* (STFT) is a modification of the Fourier transform. STFT has adapted by *Dennis Gabor* (1946), to analyze a small section of the signal at a time, a technique is called *windowing* a signal. Fig. 4.2(a) shows transformation of a signal into two-dimensional function of time and frequency. Mathematically the STFT, with window function $w(t-\tau)$ is expressed as

$$STFT(\omega) = \int_{-\infty}^{\infty} f(t).w(t-\tau).e^{i\omega t}.dt$$

where, $w(t-\tau)$ is the analysis filter or analysis window. The STFT represents a compromise between the time-domain and frequency-domain views of a signal. It provides information about frequency content in the window of the signal at the given

time. However, this information is obtained with limited precision, and that precision is determined by the size of the window. The drawback is that once a particular size is chosen for the time window, that window is the same for all frequencies. Many signals require a more flexible approach, where the window size can vary to determine more accurately in either time-domain or frequency-domain.

## 4.3 WAVELET ANALYSIS (WA)

*Wavelet Analysis* is the next logical step in which the windowing technique with variable sized regions is used. Wavelet analysis allows both low frequency information with long time intervals and high frequency information with shorter regions. Fig. 4.2(b) shows that wavelet analysis does not use a time-frequency region, but rather a time-scale region. Mathematically, the *Wavelet Transform* (WT) of a signal is defined as follows: (Legendre et al [11])

$$W_f(a,b) = \int_{-\infty}^{\infty} f(t).\frac{1}{\sqrt{a}}\psi\left(\frac{t-b}{a}\right).dt$$

where, $\psi(t)$ is a mother wavelet, $b$ is a time shift parameter and $a$ is a scaling parameter. By definition, the WT is the correlation between the signal and set of basic *Wavelets*. Wavelet analysis produces a time-scale view of a signal, with scaling and shifting. *Scaling* a *Wavelet* means stretching (or compressing) it. Fig. 4.3 shows wavelets with different scaling parameters. Shifting a Wavelet simply means delaying (or hastening) its onset. Mathematically, delaying a function $f(t)$ by $\tau$ is represented by $f(t-\tau)$. Fig. 4.4 shows wavelets with different shift factors.

Wavelet analysis is capable of revealing aspects of data that other signal analysis techniques miss such as trends; break down points, discontinuities in the higher derivatives and self-similarity. Wavelet analysis can *compress or de-noise* a signal without appreciable degradation.

Wavelet analysis can be performed in two ways

1. Using continuously translated and dilated versions of mother wavelet (CWT), or
2. Using discretely translated and dilated versions of mother wavelet (DWT).

### 4.3.1 Continuous Wavelet Transform (CWT)

The continuous wavelet transform (CWT) is defined as the sum over all time of the signal multiplied by scaled and shifted versions of the wavelet function $\psi$, which can be represented as

$$C(a,b) = \int_{-\infty}^{\infty} f(t)\psi^{*}_{a,b}(t)\ dt$$

Where, C (a, b) are the coefficients of the wavelet transform, f *(t)* is the signal being analyzed and * denotes the complex conjugate of $\psi_{a,b}$. Here, $\psi_{a,b}$ is the shifted and scaled version of the mother wavelet $\psi(t)$ as given by,

$$\psi_{a,b} = a^{-1/2}\psi\left(\frac{t-a}{b}\right),\ (a,b) \in R^2,\ a > 0$$

The word continuous in CWT means, that the transform operates the wavelets on the signal with continuous in scaling and shifting. During the computation, the analyzing wavelet is shifted smoothly over the full domain of the analyzed signal/function.

### 4.3.2 Discrete Wavelet Transform (DWT)

Calculating Wavelet coefficients in CWT at every possible scale generates a very large amount of data. This disadvantage of CWT is overcome by choosing scales and positions based on powers of two, so called dyadic scales and position, which is more efficient and just as accurate. Such an analysis is called Discrete Wavelet Transform (DWT). The generation of the wavelets and calculation of the DWT are well matched to digital computer. The wavelet transform can also be expressed in discrete form

$$f(t) = A\sum_{m}\sum_{n} C_{m,n}\psi\left(\frac{t - na_0^m T}{a_0^m}\right)$$

where,

$$C_{m,n} = a_0^{-m/2}\int f(t).\psi\left(\frac{t - na_0^m T}{a_0^m}\right).dt$$

$$a = a_0^m$$

$$b = na_0^m T$$

where, T is the sampling period, A and $a_0$ are constants, where $a_0$=2 for the dyadic wavelet transform, m is depend upon the number of decomposition levels and n is depend upon the length of the signal to be decomposed.

### 4.3.3 Multi Resolution Analysis (MRA)

Multi resolution wavelet analysis allows the decomposition of a function/signal in progression of successive *approximation* and *details*, corresponding to different scales. The *approximations* are high-scale, low frequency components and the *details* are the low-scale, high frequency components of the signal. The difference between the actual signal and its approximation of order n is called its *residual*. Intuitively, the *approximation* is relatively smooth, and *detail* being composed of high frequency components. The *detail* corresponds to the difference between two successive levels of approximation.

### 4.3.4 Multiple-Level Decomposition

In DWT, the decomposition process can be iterated, with successive approximations being decomposed in turn, so that one signal can be broken into many lower-resolution components. This is called the *Wavelet decomposition tree*. Fig. 4.5 shows the Multi-level (three level) wavelet decomposition tree.

### 4.3.5 Wavelet Reconstruction

*Wavelet reconstruction*, or *synthesis* is the process of reconstructing the decomposed signal using a set of decomposed coefficients. The mathematical manipulation that affects synthesis is called the *inverse discrete wavelet transform* (IDWT).

### 4.3.6 Properties of Wavelets

The best-performing *mother wavelet* should have the following three properties.

1. The admissible condition is given by

$$\int_{-\infty}^{\infty} \psi(t)\, dt = 0$$

2. The wavelet has the characteristic of good time-frequency localization. This property makes the wavelet transform is powerful tool for analysis of non-stationary signals such as sound, seismic, electromagnetic signals etc.
3. The power spectrum of the wavelet is well matched with that of the signal to be analyzed.

### 4.3.7 Different types of Wavelets

A wavelet is a waveform of limited duration, which has the above properties. Different types of mother wavelets are discussed in the following paragraphs.

The simplest wavelet is *Haar* wavelet, which is a step function (Figs. 4.6(a) and 4.6(b)). Ingrid *Daubechies*, invented what are called compactly supported orthonormal wavelets. The names of the *Daubechies* family wavelets are written as *dbN*, where N is the order, and *db* is the "surname" of the wavelet. The *db1* wavelet is same as *Haar*. Figs. 4.6(c) through 4.6(p) shows the scaling and wavelet functions of the various Daubechies wavelets. In *Biorthogonal* wavelets two types of wavelet functions are used: one for decomposition and other for reconstruction instead of the same one. *Coiflets, Symlets, Morlet, Mexican Hat, Mayer* etc. are other different type of wavelets suitable for various purposes.

There are different wavelets that can be used to decompose the signal and extract feature vector. These wavelets include Daubechies (db1-db10), Biorthogonal (bior1.3-bior6.8), symlets (sym2-sym8), coiflets (coif1-coif5), Morlet, Mexican hat and Meyer. The criterion for selection of the proper mother wavelet is based on the shape of the wavelet function, which could match well with the shape of the signal mode to be analyzed. In the present work, Coiflets, order 5 ('coif5') has been chosen, because it seems to match with the signal mode to be analyzed and also it possesses good time-frequency localization. Figs. 4.6(a) to 4.6(q) shows different type of wavelet and scaling functions. Fig. 4.6(q) shows the Coiflets-1 to 5 ('coif5' has been used in the present work.)

## 4.4 NOISE SUPPRESSION

In Ultrasonic Nondestructive Evaluation (NDE), the observed ultrasonic signal *S (t)* can be expressed as the sum of the two components.

$$s(t) = y(t) + n(t)$$

where, *y(t)* is the signal of the defect and *n(t)* is the noise. Noise removal is extremely important in the ultrasonic defect detection to identify the defects correctly. Optimal de-noising requires a more subtle approach called thresholding. This involves discarding only the portion of the details that exceeds a certain limit.

The main steps of the signal noise removal are.

1. Decomposition of the signal into coefficients,
2. Separation of the *approximation* and *detail* coefficients from the coefficients, and
3. Reconstruction of the de-noised signal from the *approximation* coefficients and their different levels of the noises from the *detail* coefficients.

A code for the noise suppression from the signal is available in Matlab GUI. This gives the user options for variable Thresholding, like, fixed thresholding, heuristic sure, rigorous sure, mini-max, penalize high, penalize medium, penalize low. It also facilitates selection of noise structure to be removed, i.e., unscaled white noise, scaled white noise and non-white noise. The signal received in our case from laser as well as conventional ultrasonic setups was found to have unscaled white noise, this option was used alongwith fixed thresholding facility available in GUI of Wavelet toolbox in Matlab and all signals were de-noised before compression.

## 4.5 FAST FOURIER TRANSFORM (FFT)

FFT is a powerful tool for analyzing and measure signals. FFTs are useful for measuring content of stationary transient signals and also produce the average frequency content of a signal over the entire time that the signal was acquired. FFT is a highly efficient algorithm for calculation of Discrete Fourier Transform (DFT) of finite duration sequences. The principle on which FFT is based is as follows

Let x[n] be a signal that is 0 outside the interval $0 \le n \le N_1-1$. For $N \ge N_1$, the N point DFT of x[n] is given by

$$X[k]=\frac{1}{N}\sum_{k=0}^{N-1}x[n]\ \ e^{-jk(2\pi/N)n},\ k=0, 1, 2, 3, N-1.$$

It is convenient to write above equation as

$$X[k] = \frac{1}{N}\sum_{k=0}^{N-1} x[n]W_N^{nk}$$

Where

$$W_N=\cos(2\pi/N)-j\sin(2\pi/N)$$
$$=e^{-j2\pi/N}$$

When N is a power of two, $N=2^m$, this iterative step may be used m times to yield the Fourier coefficients without using matrix multiplication. The fast Fourier transform requires only $N\log_2 N$ operations instead of $N^2$ operations. By making a changes the basic FFT algorithm may also be used to compute the inverse FFT. Since fewer computations are required, the amount of round-off error is also reduced. The speed of the FFT algorithm makes it practical to use it in various types of digital analysis including: clear ultrasonic images, reduction of noise, Autocorrelation function estimation, Cross-correlation function estimation, power spectrum estimation, Harmonic analysis and synthesis, numerical solution of defferential equations. It is also evaluated by using the interference phenomenon, even when the dimensions desired are smaller than the ultrasonic wavelength.

### 4.5.1 Amplitude Spectrum

As the recorded signal is dominated by a sinusoidal rhythm, the easiest way to analyze these data is by performing an analysis called Fourier analysis. Calculating the Fourier transform is equivalent to calculating the contribution to the analyzed signal of sine waves of different frequencies. These calculations were done by FFT using MATLAB. After computing the Fourier transform, the signal has been transformed from the time domain to the frequency domain, where the x-axis is now frequency instead of time, and

the y-axis is the contribution (amplitude) of that frequency component. This waveform is also called amplitude spectrum.

The FFT returns a two-sided spectrum in complex form (real and imaginary parts), which must scale and convert to polar form to obtain magnitude and phase. The amplitude of the FFT is related to the number of points in the time-domain signal. The following equation was used to compute the amplitude verses frequency from the FFT.

$$\text{Amplitude spectrum in quantity peak} = \frac{Magnitutude[FFT(A)]}{N}$$

$$= \frac{\sqrt{[real[FFT(A)]]^2 + [imag[FFT(A)]]^2}}{N}$$

Where

A, denotes the signal in time-domain.

N, denotes the length of the amplitude spectrum

### 4.5.2 Average Signal Power (Parseval's relation)

Power is always in physical units of energy per unit time. It therefore makes sense to define the average signal power as the total energy divided by its length. Normally signals are functions of time and the total energy of a signal is defined using the time domain description of the signal. In the present work, the total energy of a signal calculated using the Fourier Transform of the signal.

Consider a signal A(t) over the entire interval $-\infty$ t $< \infty$ and let it assumed that its Fourier Transform A($j\omega$) exists. Then the Parseval's relation is given by

$$\int_{-\infty}^{\infty} |A(t)|^2 dt = \frac{1}{2\pi} \int_{-\infty}^{\infty} |A(j\omega)|^2 d\omega$$

Where the term on the left hand side of the above equation is the total energy of the signal A(t). Parseval's relation says that this total energy may be determined either by computing the energy per unit time $\left(|A(t)|^2\right)$ and integrating over all time or by computing the energy per unit frequency $\left(|A(j\omega)|^2 / 2\pi\right)$ and integrating over all

frequencies. For this reason, $\left(|A(j\omega)|^2\right)$ is often referred to as the energy-density spectrum of the signal A(t).

Parseval's relation for finite energy signals is the direct counterpart of Parseval's relation for periodic signals, which states that the average power of a periodic signal equals the sum of the average powers of its individual harmonic components, which in turn are equal to the squared magnitudes of the Fourier series coefficients. Mathematically,

$$\frac{1}{T}\int_T |A(t)|^2\,dt = \sum_{k=0}^{N-1} |A_k|^2$$

Where T is the period of the signal.

$A_k$ are Fourier series coefficients (amplitude spectrum) of A (t).

## 4.6 CLOSURE

In this Chapter, Signal Processing techniques like FT, STFT, FFT etc and later day techniques like Wavelet Transform (WT) have been presented with special reference to their role in laser based ultrasonics. Some of the important mother wavelets and their properties have been discussed. Noise removal using multi-level DWT, which has been used in the present work, has also been explained.


Fig. 4.1 Fourier Transform for transforming a time-domain signal to frequency-domain

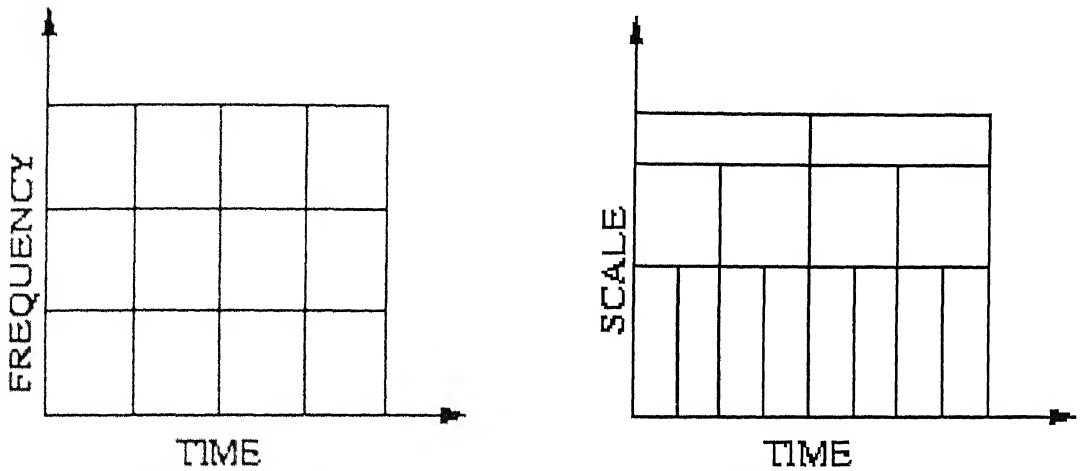


(a) STFT (Gabor) (b) Wavelet Analysis

Figs. 4.2(a-b) Short-Time Transform (Time-frequency domain), Wavelet Transform (Time-scale domain)

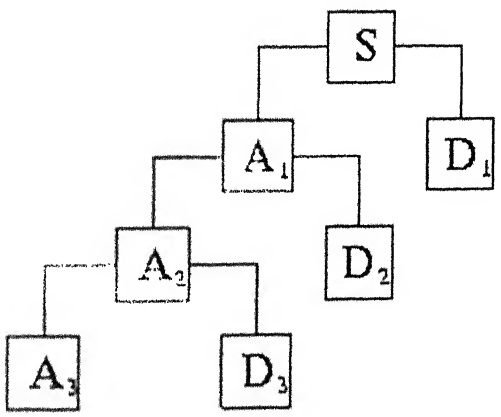


$$S = A_1 + D_1$$

$$= A_2 + D_2 + D_1$$

$$= A_3 + D_3 + D_2 + D_1$$

Fig. 4.3 Multiple-Level Wavelet decomposition tree with three-level decomposition

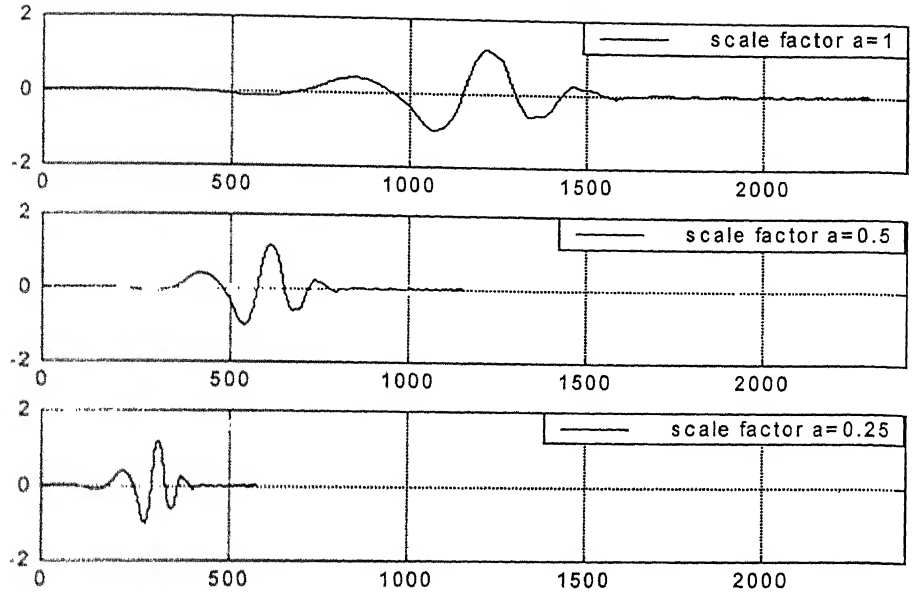


Fig. 4.4 Scaling (stretching or compression) of the wavelets with different scale factors

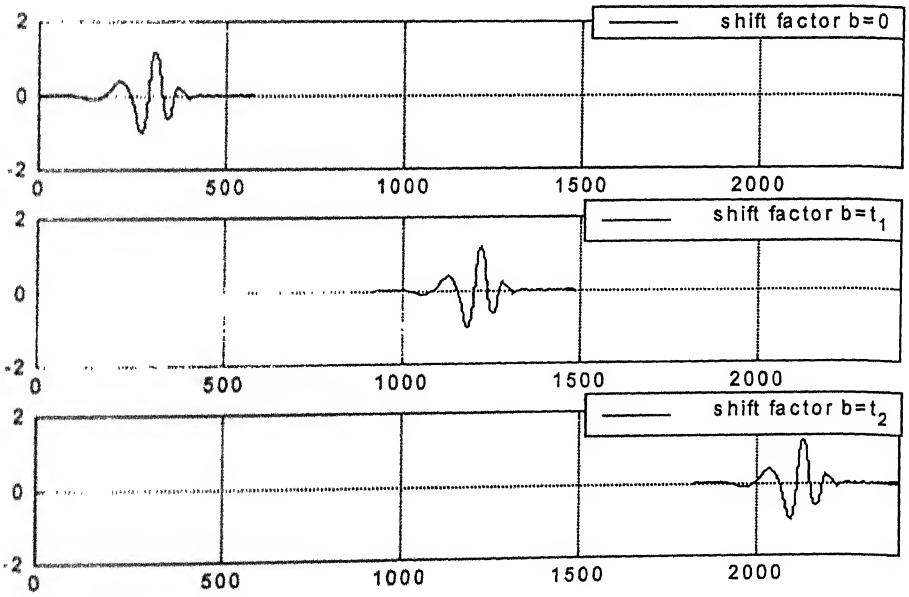


Fig. 4.5 Shifting (delaying or hastening) of the wavelets with different shift parameters

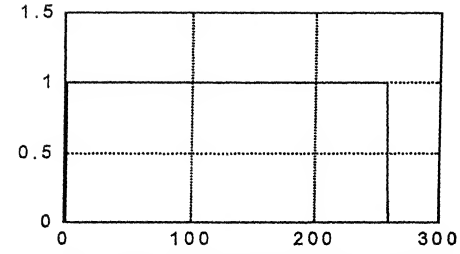


(a) db1/Haar Scaling function

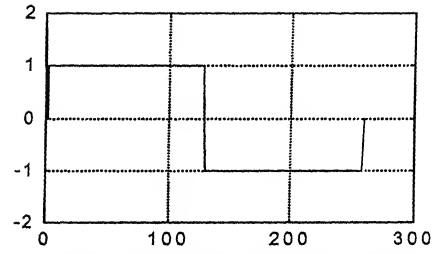


(b) db1/Haar Wavelet function

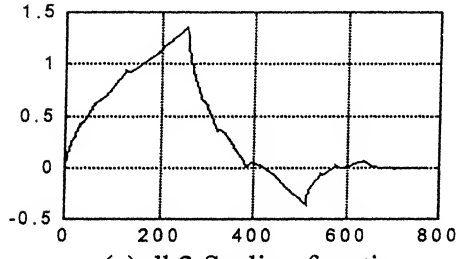


(c) db2 Scaling function

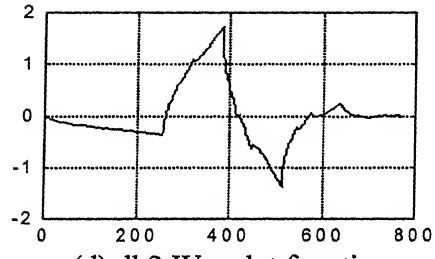


(d) db2 Wavelet function

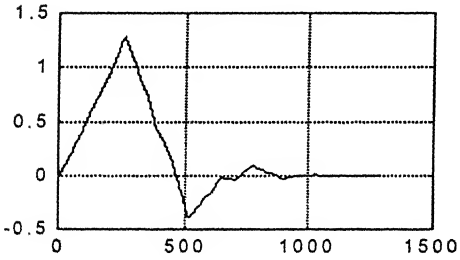


(e) db3 Scaling function

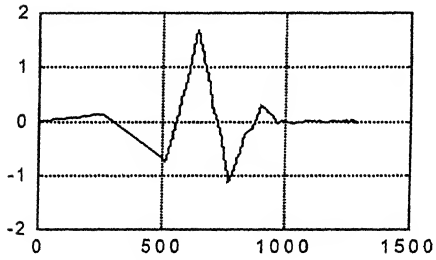


(f) db3 Wavelet function

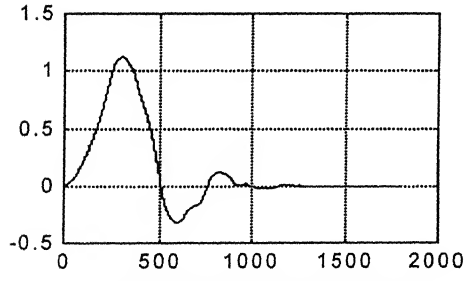


(g) db4 Scaling function

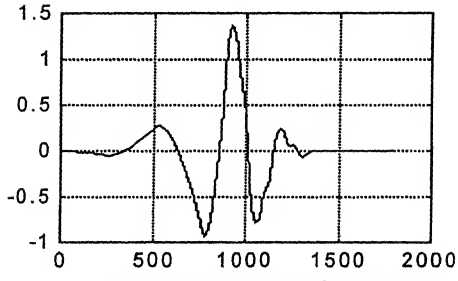


(h) db4 Wavelet function

Figs. 4.6(a-h) Different wavelets (Daubechies) scaling and wavelet functions

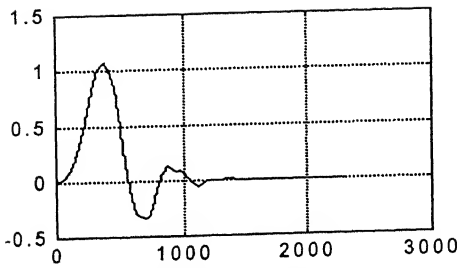


(i) db5 Scaling function

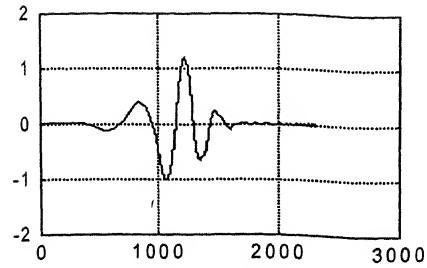


(j) db5 Wavelet function

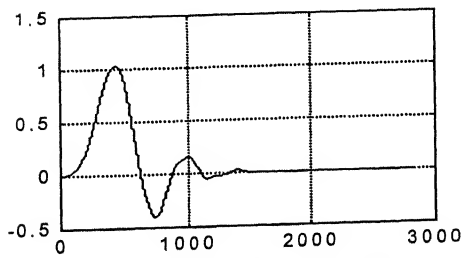


(k) db6 Scaling function

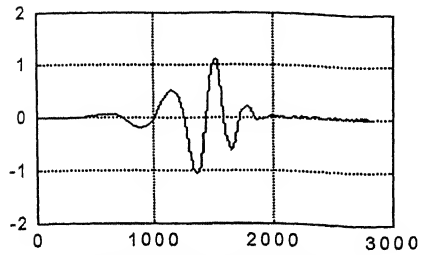


(l) db6 Wavelet function

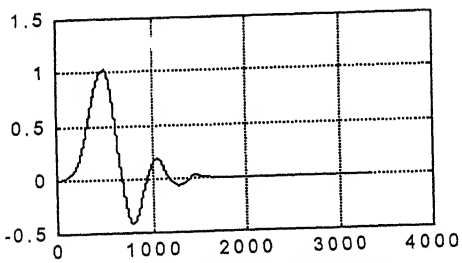


(m) db7 Scaling function

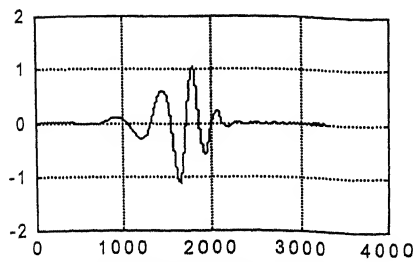


(n) db7 Wavelet function

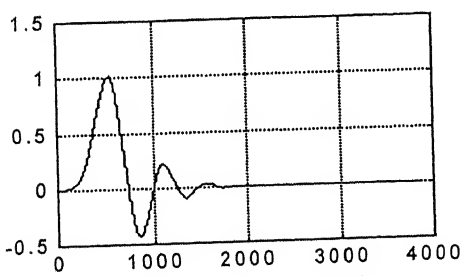


(o) db8 Scaling function

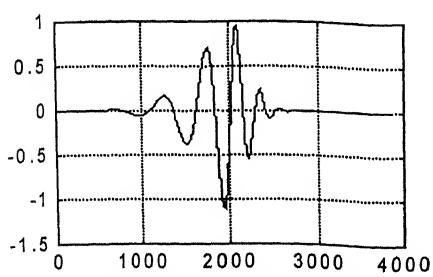


(p) db8 Wavelet function

Figs. 4.6(i-p) Different wavelets (Daubechies) scaling and wavelet functions

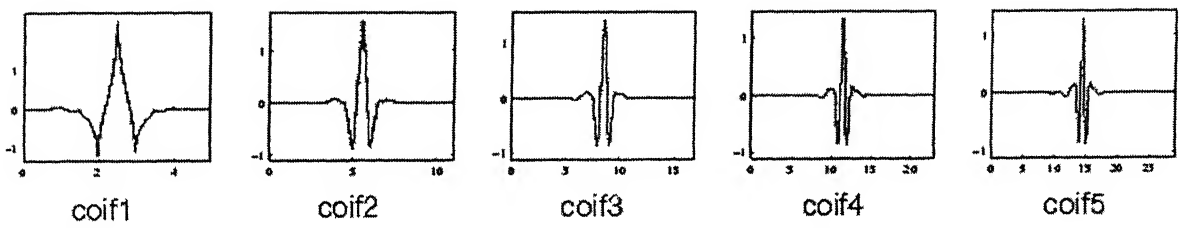


Fig 4.6(q) Coiflets in order from Coif1 to Coif5

*Chapter 5*

# RESULTS AND DISCUSSIONS

In the present study, an experimental technique has been developed using an Nd: YAG pulsed laser for generation of ultrasonic waves and a He-Ne continuous laser based heterodyne optical interferometric probe for detection. Tests were conducted on homogeneous (aluminium) and non-homogeneous (glass-epoxy unidirectional $30^0$,$45^0$,$60^0$ fiber orientation composites) specimens. Following are the results and discussions of these investigations.

## 5.1 Experimental Details

The characterization of the Nd: YAG laser beam for the purpose of ultrasonic wave generation is done using various type of slits made in a Teflon plate as explained in section 3.2. Experiments were conducted on different type of materials with various power inputs of the Nd: YAG laser beam. To obtain a good signal to noise ratio of the ultrasonic signal, the signal was averaged over four readings. FFT has been used to get the frequency components of the recorded signals.

Firstly, the knob located on the control panel to manually vary input power of the beam was calibrated. For different positions of the knob setting, the power was measured using a power meter. The values are plotted in Fig.5.1 and a best-fit straight line passing through origin was determined. The equation of the line was found to be

$$y = m*x$$

where,

Slope of the line, m = 454.19

For the rest of the analysis, this graph is made use of.

## 5.2 Power distribution within the Nd: YAG laser beam

The Nd: YAG laser beam is approximately of 7mm diameter and the power is non-uniform within this cross section. To determine spatial variation of the power, the power of the portions of beam was measured by letting the beam pass through small slits or small holes. In the present analysis, rectangular slit of 10mm x 1mm was cut in a Teflon plate which was moved across the beam and the measurements were made at discrete locations (Fig.5.2) with different power settings. Similarly, a Teflon plate with a hole of 1mm diameter was moved across the beam. The power meter readings for rectangular slit and hole are shown in Figs 5.3(a) to 5.3 (b) and the beam is found to be Gaussian in nature. From these plots it is clearly observed that the intensity of beam is maximum at center and the curve is steeper at high power settings. The Gaussian distribution function satisfied by the experimental data is given by

$$y(x) = ae^{\frac{-(x-\mu)^2}{2\sigma^2}}$$

where,

μ is the mean and

σ is the standard deviation.

The values of a, μ and σ are listed in tables 5.1(a) and 5.1(b).

Table5.1(a) Parameters of Gaussian distribution when 1mm slit is moved across the beam

| Incident Nd: YAG power in mW | a | σ | μ |
|---|---|---|---|
| 454.19 | 45.8650 | 1.9458 | 4.0000 |
| 681.28 | 91.2575 | 2.0093 | 4.0000 |
| 908.38 | 136.7885 | 2.0269 | 4.0000 |
| 1135.47 | 182.3405 | 2.0352 | 4.0000 |
| 1362.57 | 227.9003 | 2.0401 | 4.0000 |
| 1589.66 | 273.4623 | 2.0434 | 4.0000 |
| 1816.76 | 319.0200 | 2.0457 | 4.0000 |

Table5.1(b) Parameters of Gaussian distribution when 1mm hole is moved across the beam.

| Incident Nd: YAG power in mW | a | σ | μ |
|---|---|---|---|
| 681.28 | 10.0567 | 2.5362 | 4.0000 |
| 908.38 | 17.5271 | 2.3128 | 3.9999 |
| 1135.47 | 24.9961 | 2.2419 | 4.0000 |
| 1362.57 | 32.4607 | 2.2033 | 4.0000 |
| 1589.66 | 39.9253 | 2.1798 | 4.0000 |

## 5.3 Nature of ultrasonic wave generated by Nd: YAG laser

To know the nature of the ultrasonic waves generated by the Nd: YAG laser beam impinging on the specimen, ultrasonic signals on the other side of the specimen were recorded for all seven positions as explained in Section 3.2. As explained above, the pulse laser beam is made to pass through the slit (or hole) and impinge on the specimen, while the He-Ne laser was focused on to a spot right opposite the incident Nd: YAG beam location. Some typical signals in time domain on different materials are shown in Figs. 5.4(a) to 5.4(d). These signals need to be further analyzed as discussed below.

### 5.3.1 Aluminium specimen

The signals were recorded at a beam input power of 1135mW and the respective signals were plotted in frequency domain. At every location, it can be observed that the component corresponding to 79.8 KHz has the maximum value. The symmetry of the beam is observed by comparing the frequencies corresponding to higher peaks at the symmetry points. The plots are shown in Figs. 5.5 (a) to 5.5 (h). The MATLAB code used to obtain these curves is given in Appendix E.

Average power of each signal was calculated from Parseval's relation using the code developed in MATLAB (Appendix E). Figs.5.6 (a) and 5.6 (b) show the ultrasonic power distributions for Nd: YAG laser passed through 1 mm slit or 1 mm diameter hole respectively. The response of the beam is also found to be Gaussian in nature. From the

plot it can be observed that at low power settings beam intensity is more uniformly distributed while at higher power settings central portion of the beam has far more power.

### 5.3.2 Unidirectional Glass-epoxy composite specimen

Figs.5.7 (a) to 5.7 (c) show the variation of strength of ultrasonic wave generated on $30^0$,$45^0$ and $60^0$-glass-epoxy composite specimens respectively. The response of the beam is also found to be Gaussian in nature. From the plots it can be observed that for all power settings, $30^0$ and $60^0$-specimens behave in the same way. For $45^0$-specimen, at low power settings beam intensity is more uniformly distributed, while at high power settings central portion of the beam has far more power. The strength of ultrasonic signal is found to be higher in case of glass-epoxy composite specimens as compared to the aluminium specimen. This may be attributed to the opaqueness of aluminium than glass-epoxy composites.

## 5.4 Axisymmetric beam portion

### 5.4.1 Circular beam

The beam was passed through holes of 1mm, 2mm and 3mm diameters. Power per unit area was calculated from power meter readings before specimen. Fig.5.8 (a) shows the variation of incident beam power spatial density as beam diameter is increased, for different input beam power settings. From the plot it is clear that incident beam power spatial density increases with increase in beam diameter. The strength of ultrasonic signal was calculated from the signals for different power settings. Fig. 5.8 (b) shows the variation of strength of ultrasonic signal/cross sectional area of incident Nd: YAG laser beam as beam diameter is increased. From the plot it is observed that attenuation rate decreases with increase in beam diameter. Fig.5.8(c) shows the variation strength of signal/ cross sectional area of incident Nd: YAG laser beam with incident beam power spatial density for different input power settings.

### 5.4.2 Circumferential slits

The beam was passed through circumferential slit of 1mm width at mean radii 4mm, 5mm, and 6mm. Power per unit area was calculated from power meter readings before

impinging on the specimen. Fig.5.8 (d) shows the variation of incident beam power spatial density as mean slit radii is increased, for different beam power settings. From the plot it is clear that incident beam power spatial density decreases with increase in mean slit radii. Then beam was allowed to impinge on the specimen after passing through the slits. The strength of ultrasonic signal was calculated from the signals for different power settings. Fig. 5.8 (e) shows the variation of strength of ultrasonic signal/ cross sectional area of incident Nd: YAG laser beam as mean slit radii is increased and it is observed that strength of ultrasonic signal / cross sectional area of incident Nd: YAG laser beam decreases with increase in mean slit radii same as average beam power.

## 5.5 Beam of High Incident Power (Ablation)

A number of different physical processes may take place when a laser beam hits a solid surface. At lower incident powers this include heating, the generation of thermal waves, elastic waves (Ultrasound). At higher powers material may get ablated from the surface and a plasma formed, while in the sample there may be melting, plastic deformation and even the formation of cracks. To know the effect of high incident power, high power laser beam was passed through a focusing lens before it falls on aluminium specimen. At incident power of 2270mW, signals were recorded for three cases viz. (a) specimen before focal length (spot diameter approximately 1.4mm), (b) specimen at focal length (spot diameter approximately 1mm) and (c) specimen after focal length (spot diameter approximately 1.3mm). Figs.5.9 (a) to 5.9(c) shows the amplitude spectrum of the above signals. From the FFT analysis, it can be observed that amplitude corresponding to any frequency is highest when the specimen is placed at focal length as compared to other two cases.

Then at incident power of 2725mW, laser beam was focused on the same specimen and vaporization of material was observed. Fig. 5.10 shows the photograph of ablated specimen. The corresponding signal was plotted in frequency domain as shown in Fig.5.11. From the plot it can be observed that at higher frequencies the amplitudes of ablation region are greater than the amplitudes of thermoelastic region. This may be due to the incident pulse power starts falling soon after the pulse gets switched off.

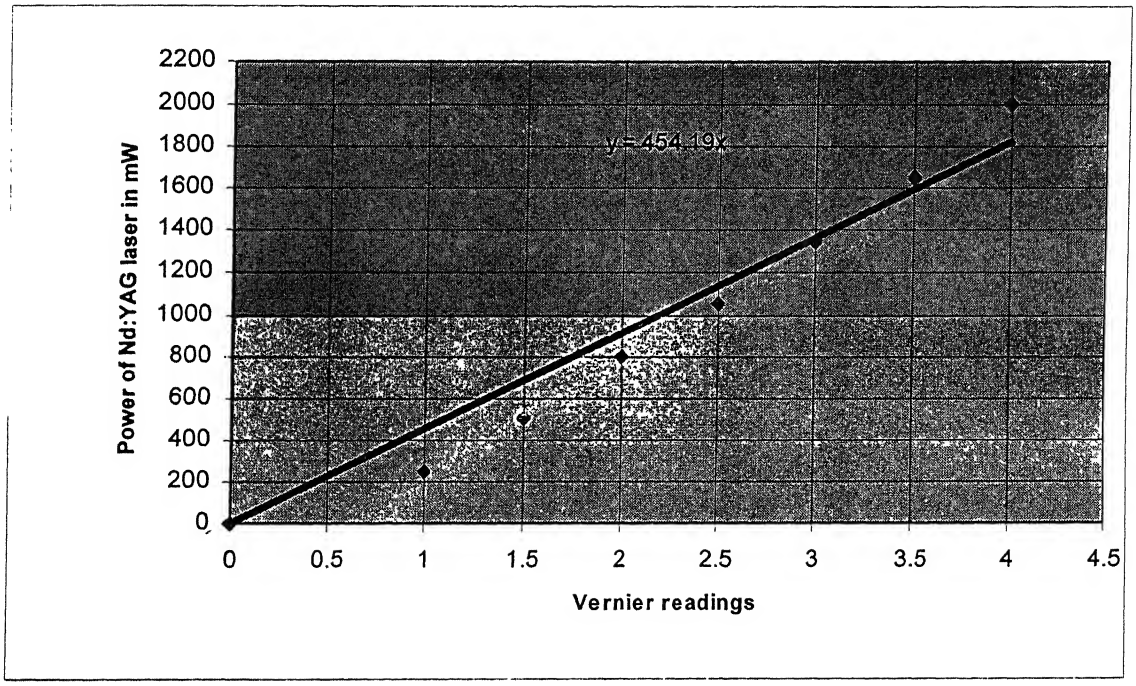


Fig.5.1 Calibration of Nd: YAG power unit

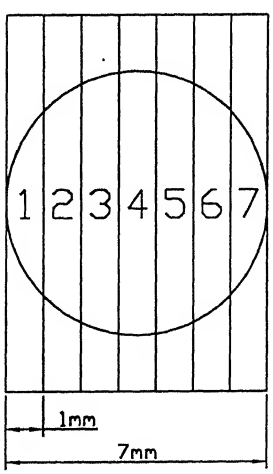


Fig.5.2 Beam of 7mm diameter

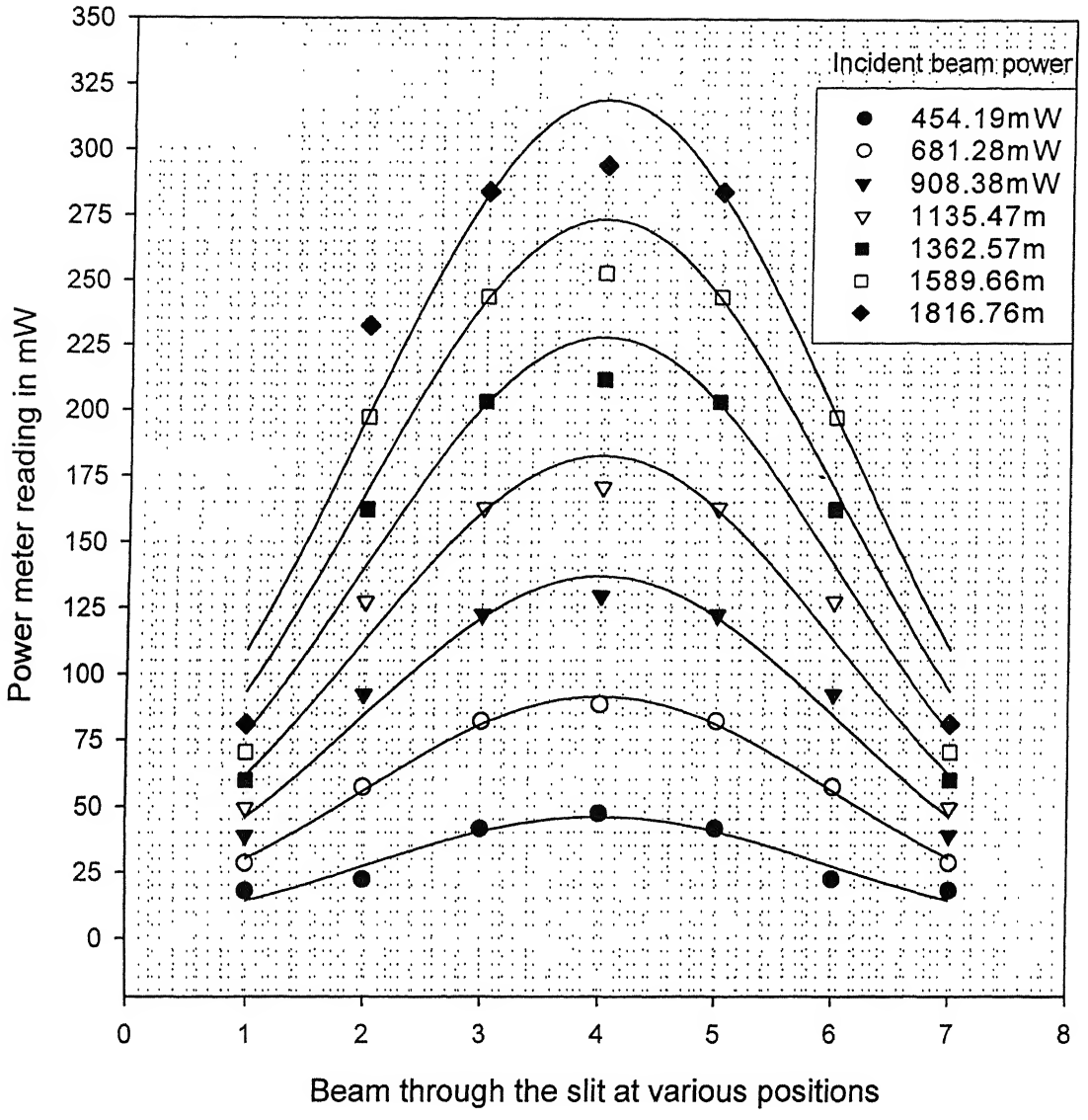


Fig.5.3 (a) Power distribution of Nd: YAG laser passed through rectangular slit.

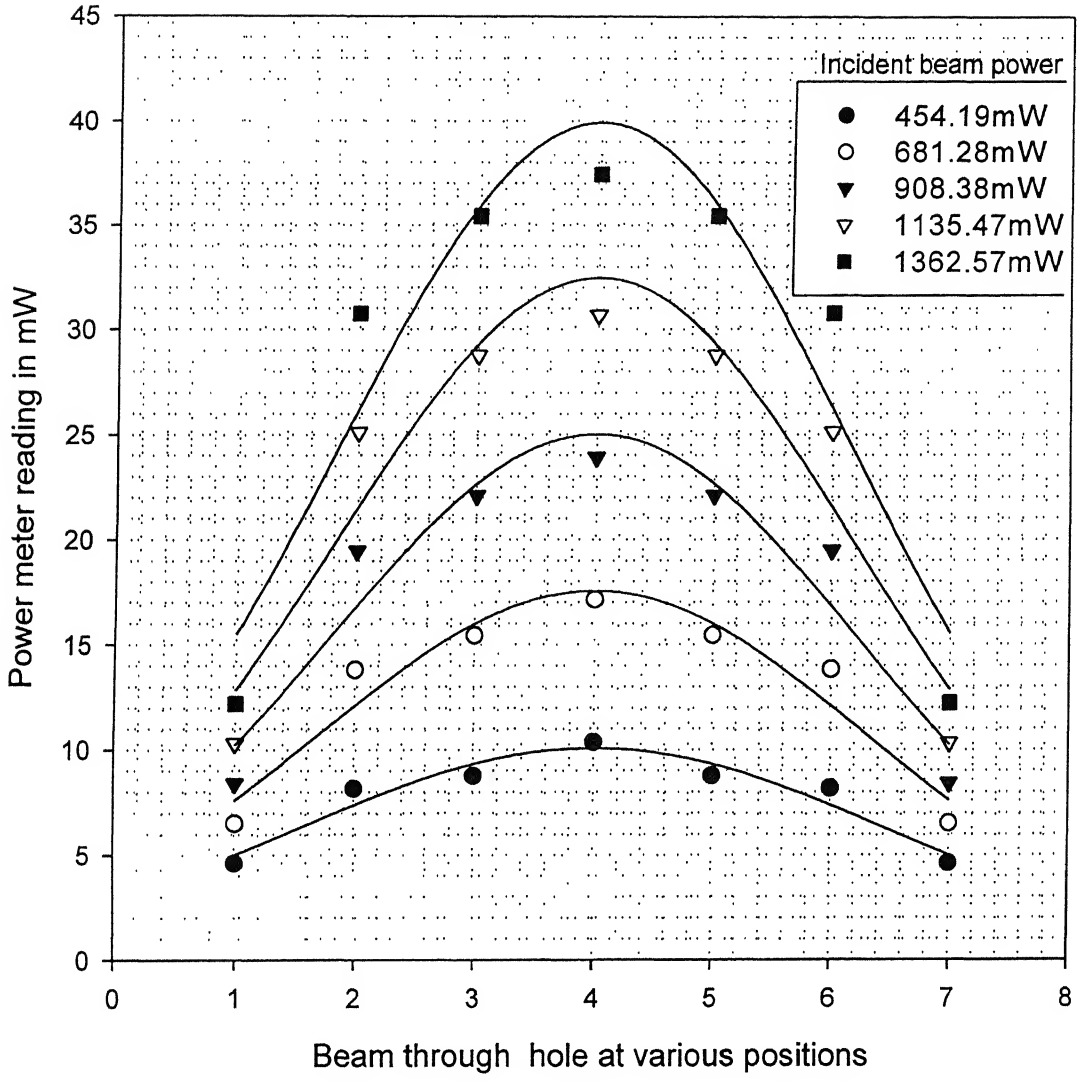


Fig.5.3 (b) Power distribution of Nd: YAG laser passed through 1mm hole.

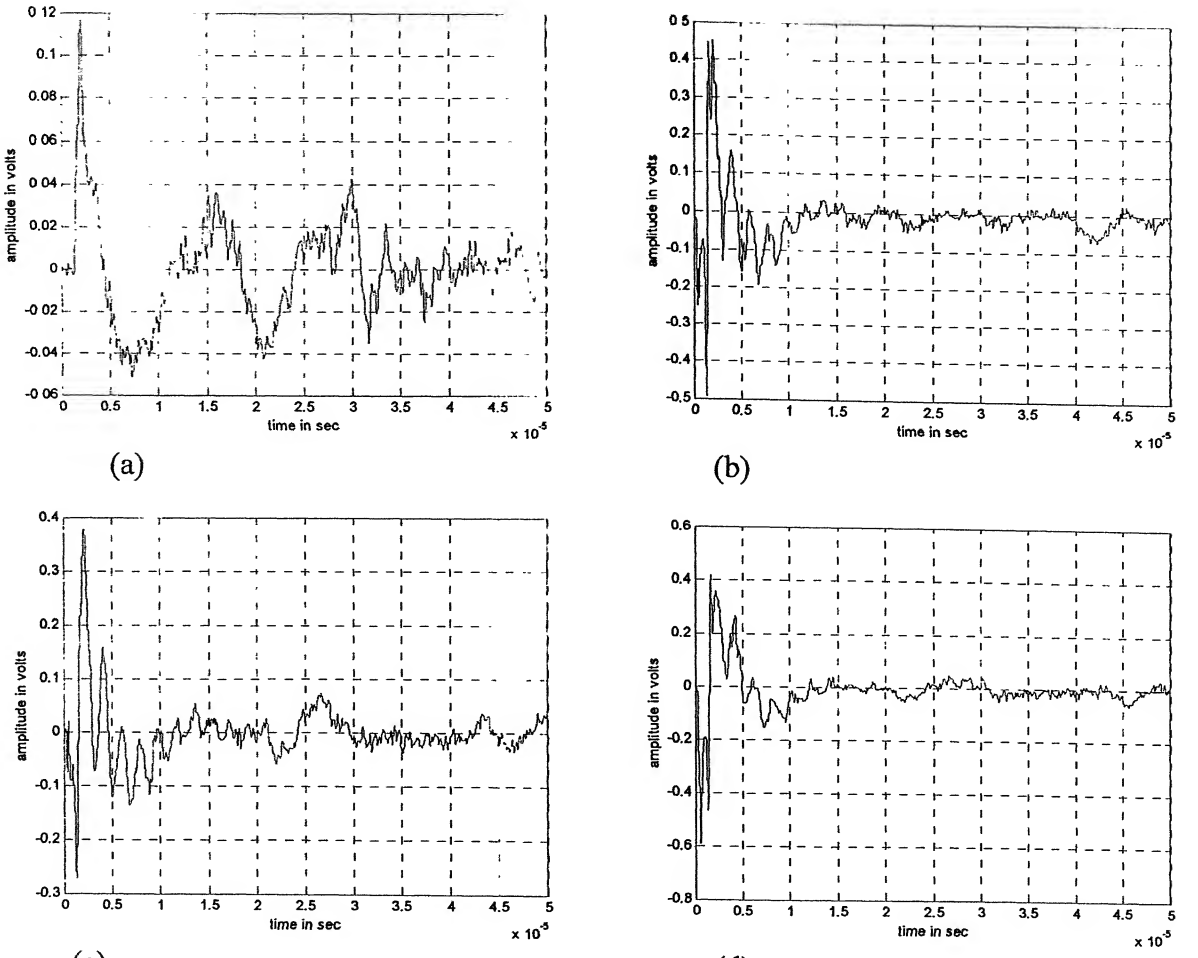


Fig 5.4. Denoised signals corresponding to (passed through rectangular slit) incident power of beam 127.143 mW
(a) Aluminium material (b) Glass epoxy unidirectional $30^0$ composite material
(c) Glass epoxy unidirectional $45^0$ composite material (d) Glass epoxy unidirectional $60^0$ composite material

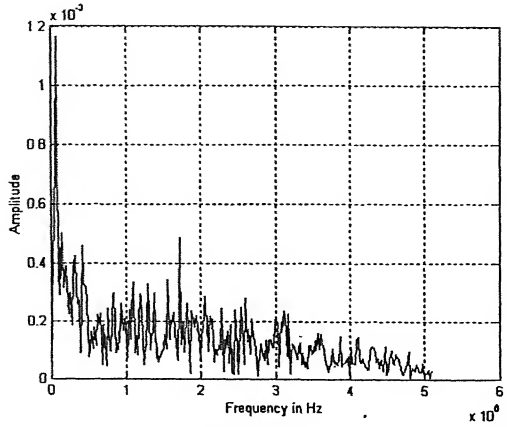


(a) At position 1

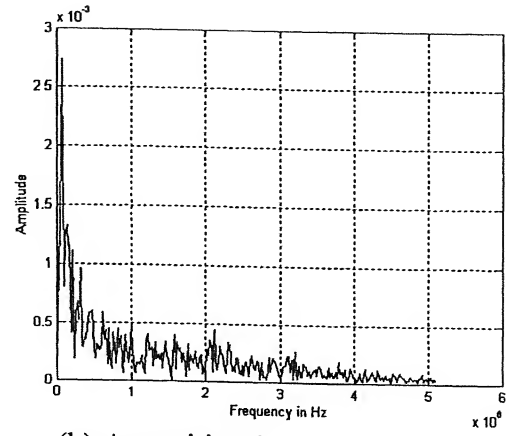


(b) At position 2

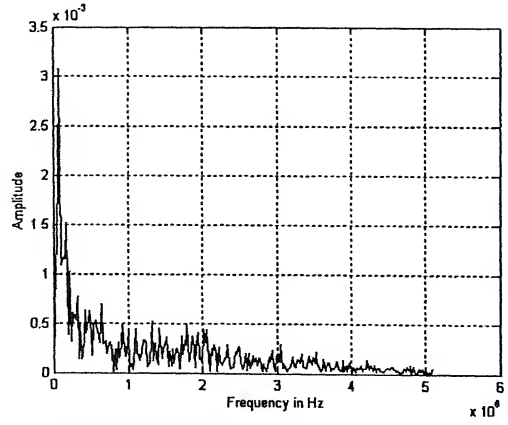


(c) At position 3

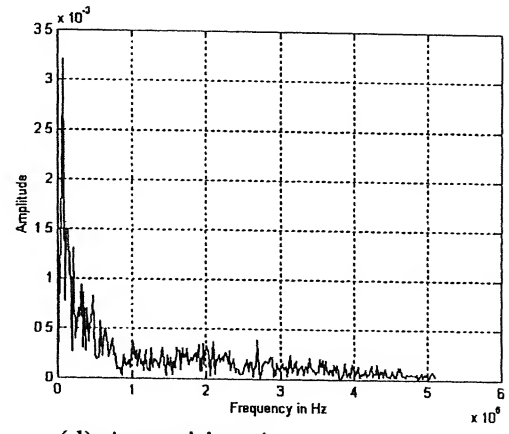


(d) At position 4

Fig.5.5 Amplitude spectrums corresponding to all positions of 1mm diameter beam at input power of 1135.47mW

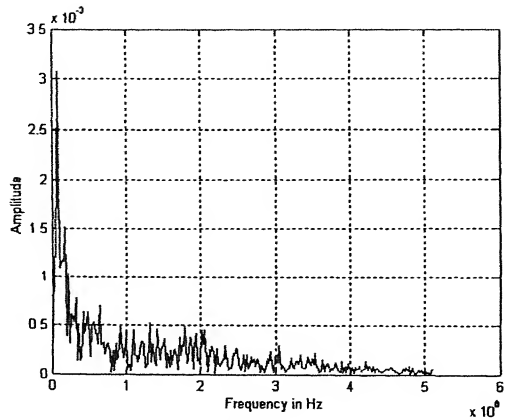


(e) At position 5

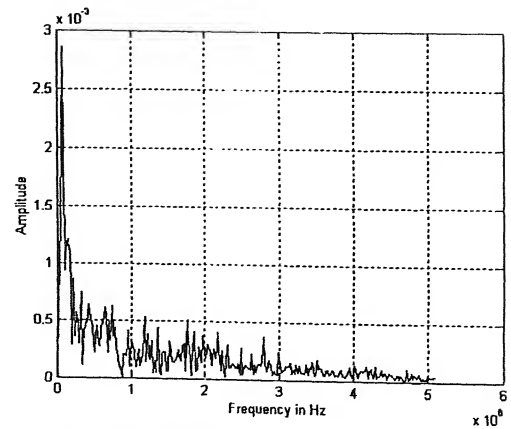


(f) At position 6

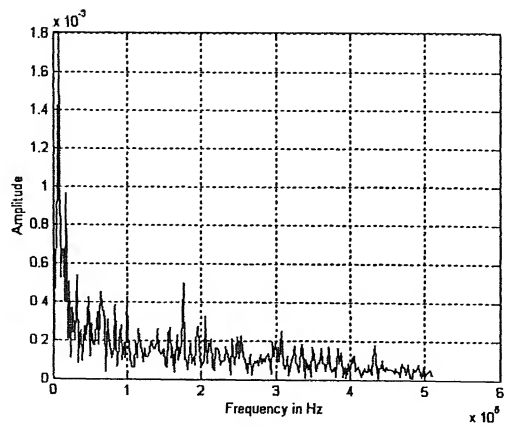


(g) At position 7

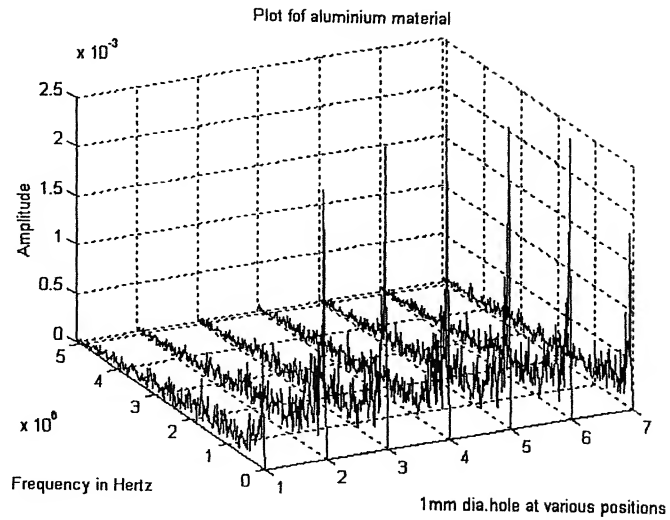


(h) 3D graph for the above

Fig.5.5 Amplitude spectrums corresponding to all positions of 1mm diameter beam at input power of 1135.47mW

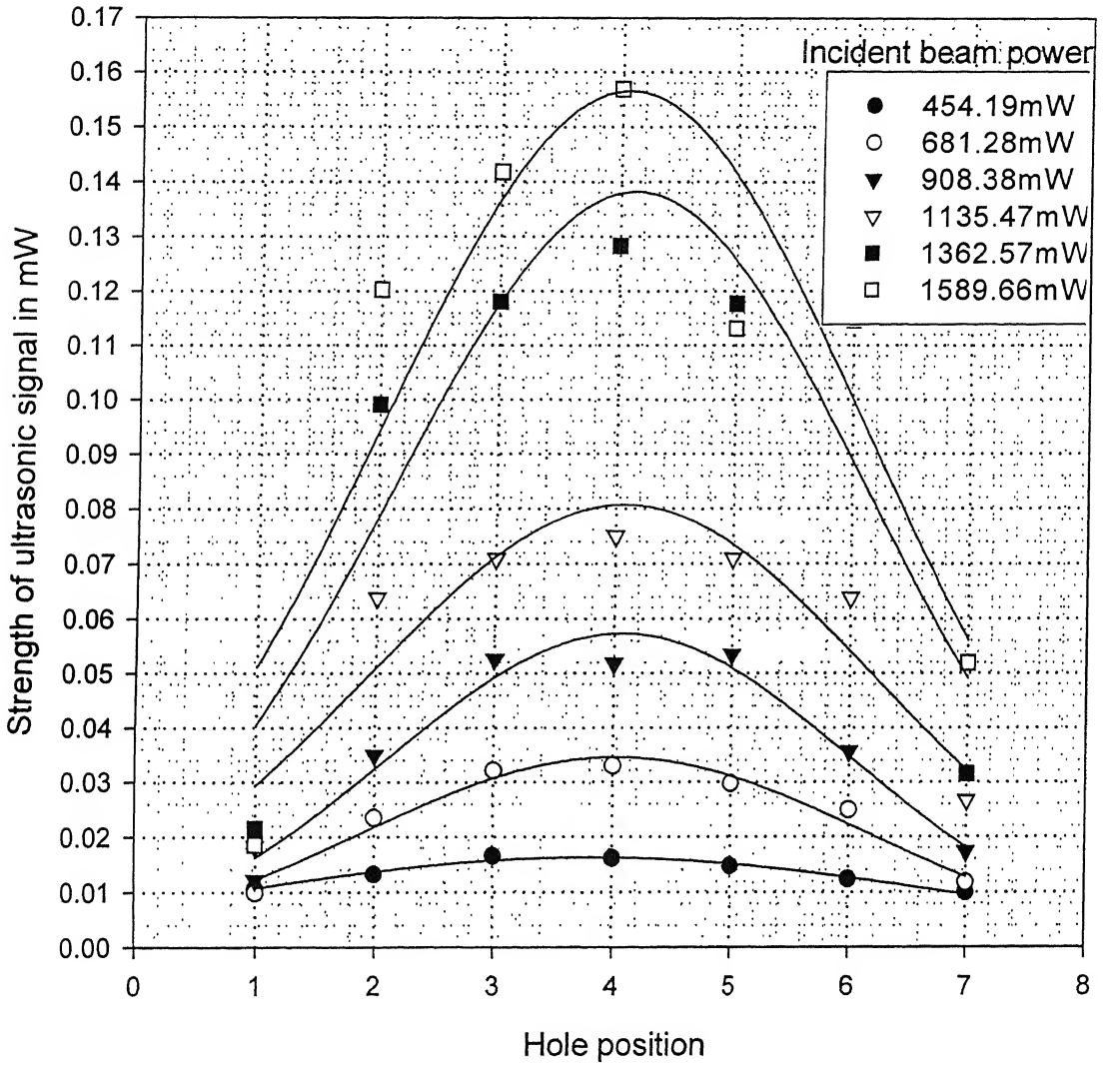


Fig.5.6 (b) Distribution of ultrasonic signal strength when Nd: YAG laser was passed through 1mm hole (material: aluminium)

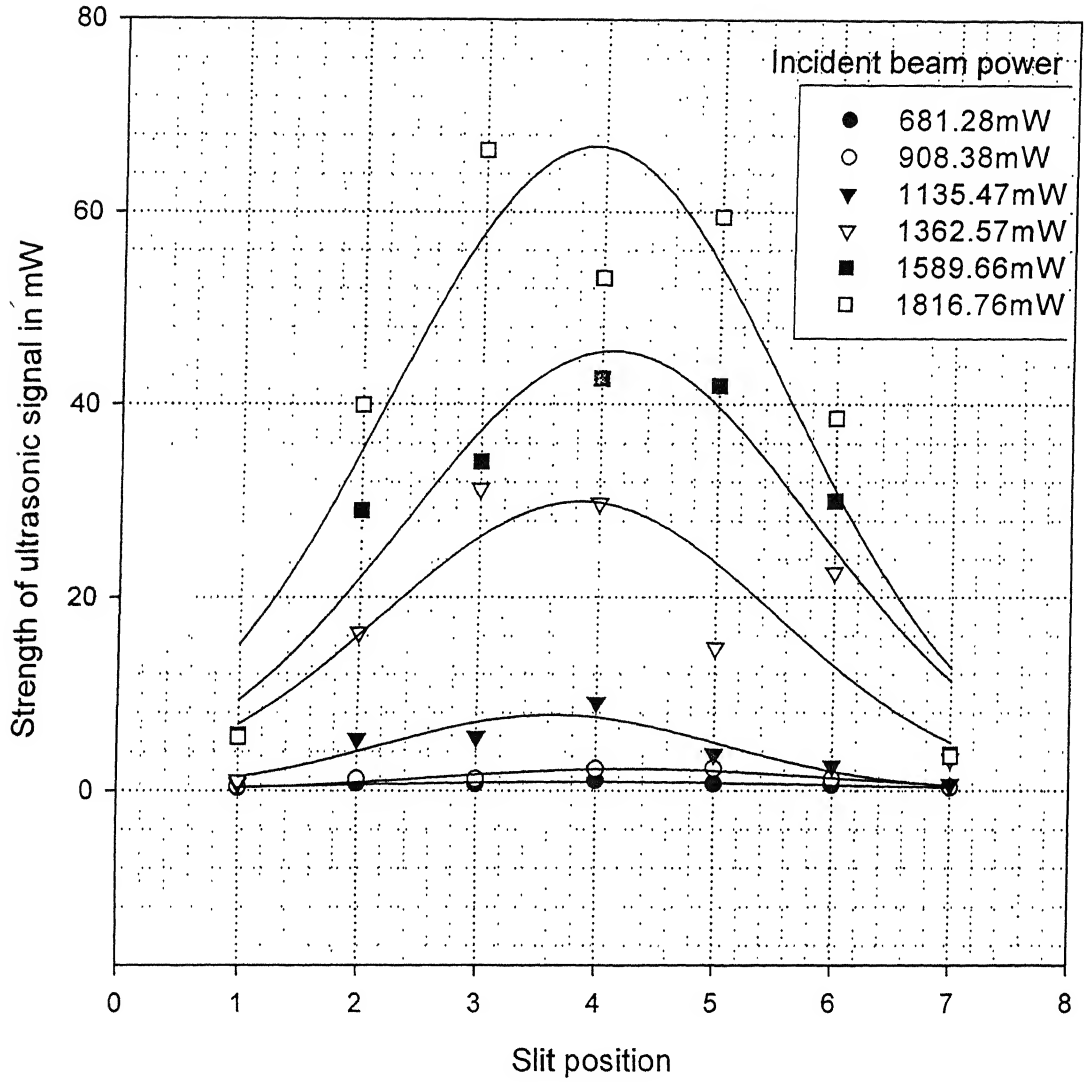


Fig.5.7 (a) Distribution of ultrasonic signal strength when Nd: YAG laser was passed through rectangular slit (material: $30^0$ unidirectional glass-epoxy composite)

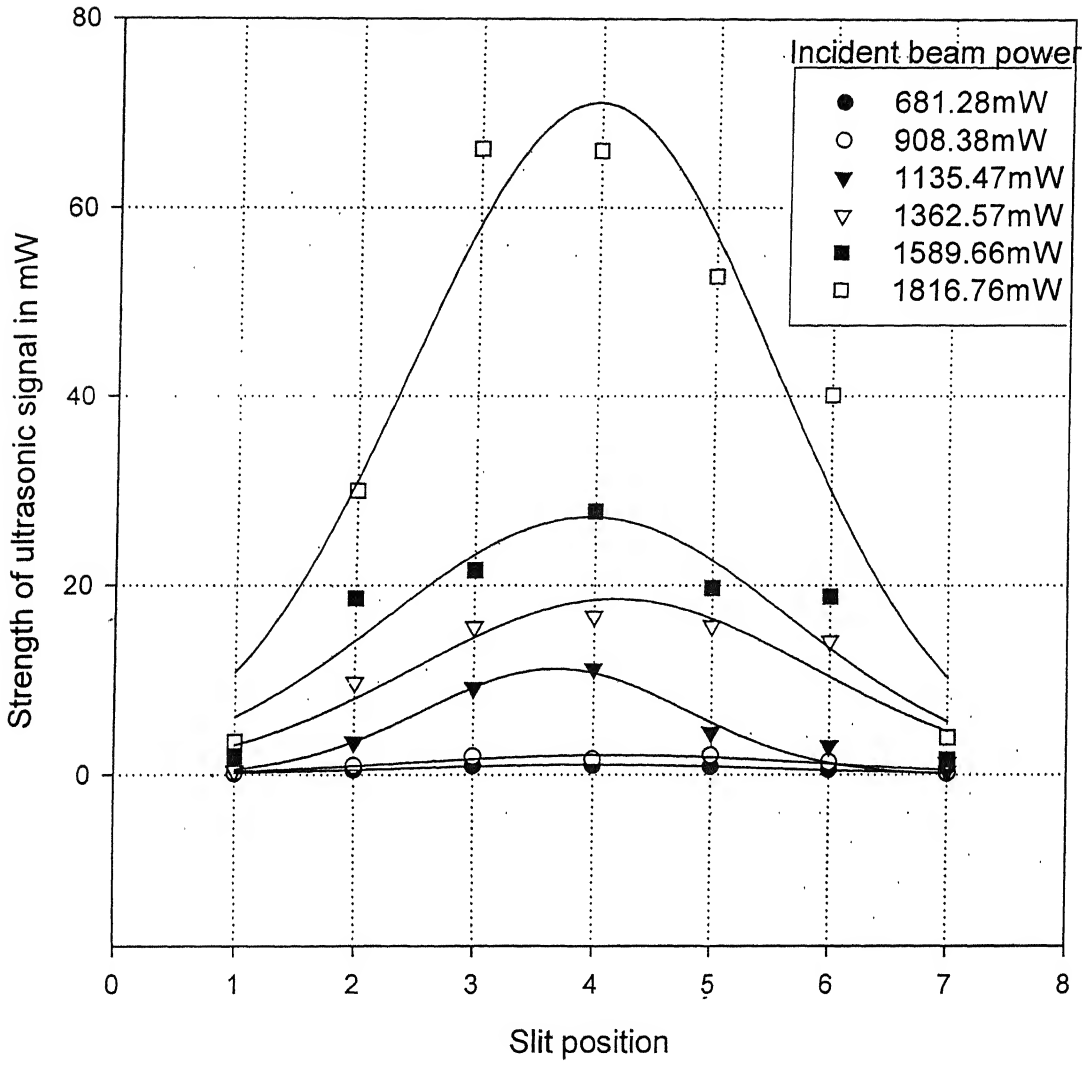


Fig.5.7 (b) Distribution of ultrasonic signal strength when Nd: YAG laser was passed through rectangular slit (material: $45^0$ unidirectional glass-epoxy composite)

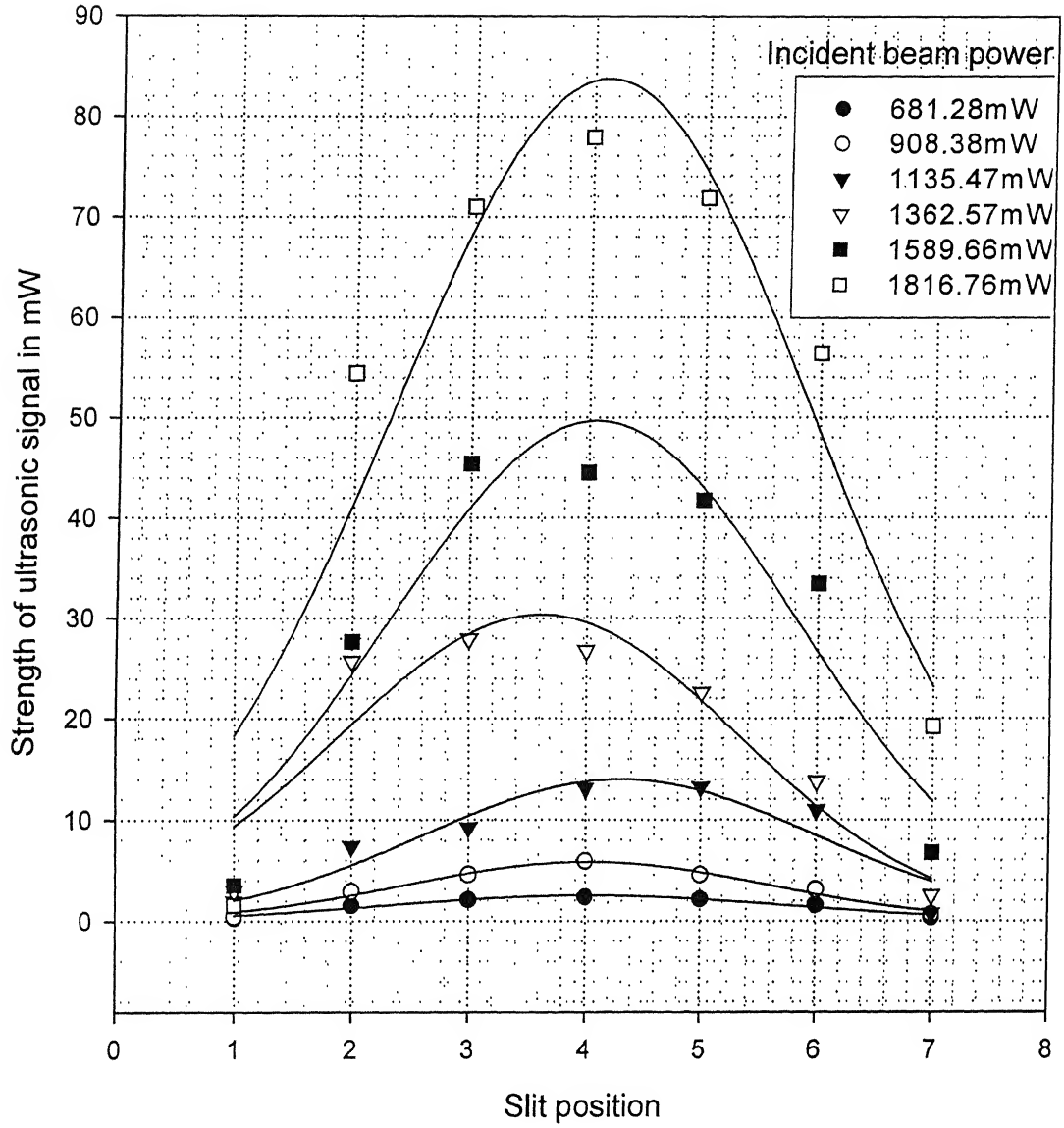


Fig.5.7 (c) Distribution of ultrasonic signal strength when Nd: YAG laser was passed through rectangular slit (material: $60^0$ unidirectional glass-epoxy composite)

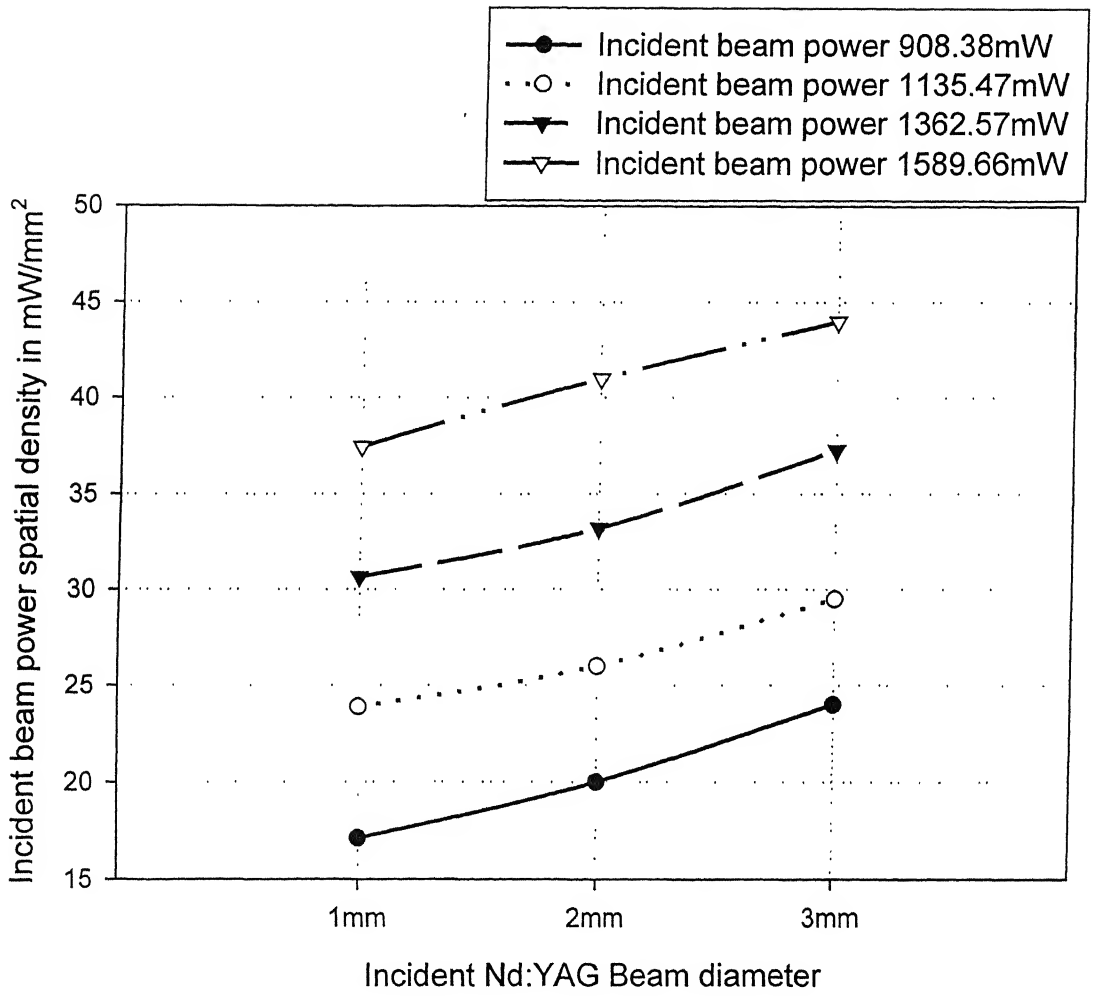


Fig. 5.8 (a) Comparison of incident beam power spatial density with increased beam diameter

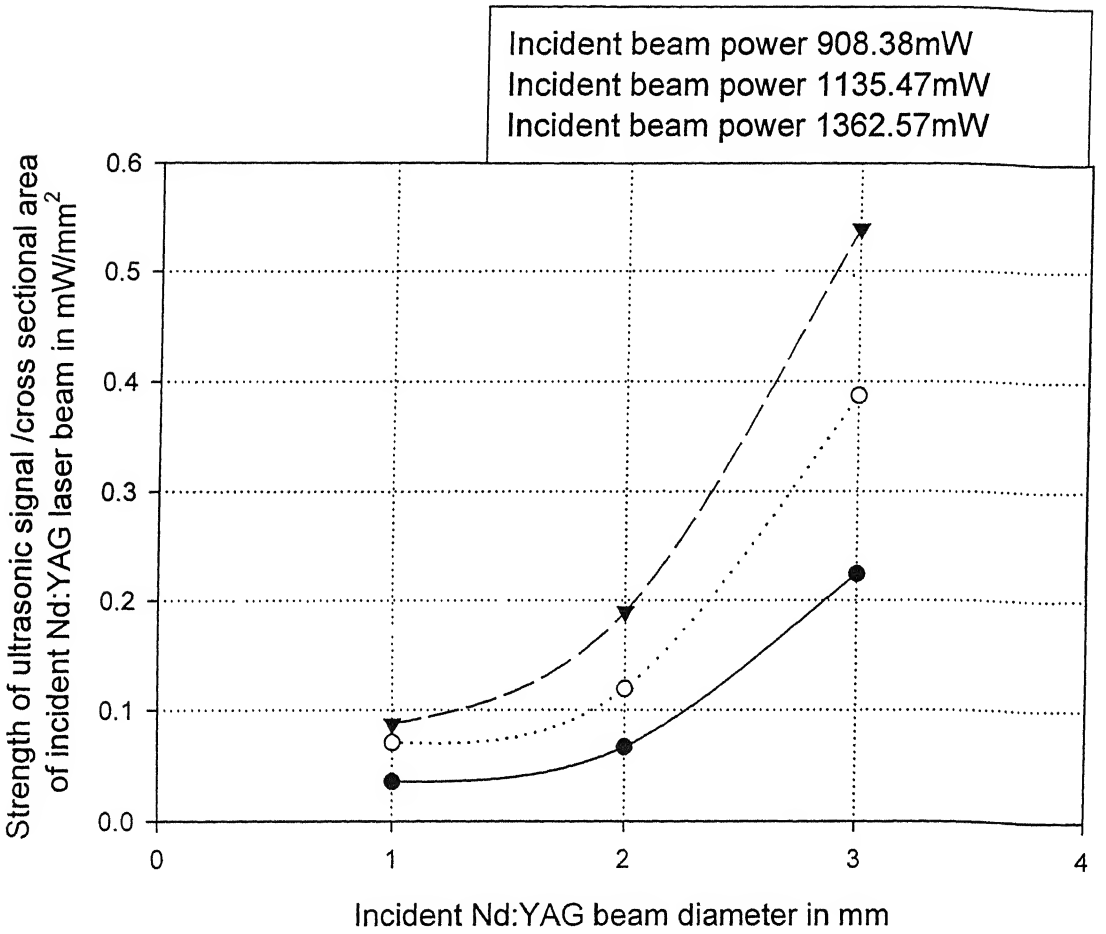


Fig. 5.8 (b) Comparison of ultrasonic signal strength/cross sectional area of incident Nd: YAG laser beam with increased beam diameter (material:aluminium)

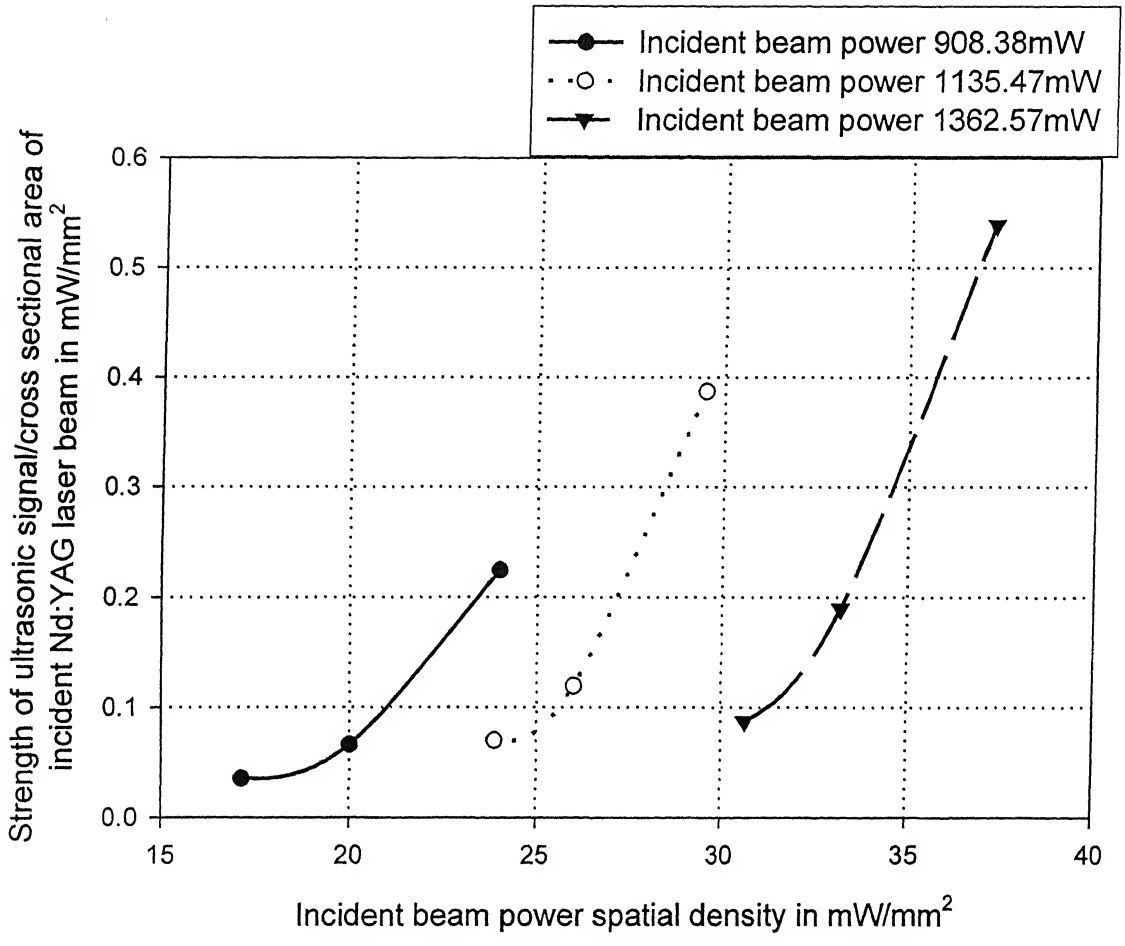


Fig.5.8(c) Strength of ultrasonic signal/ cross sectional area of incident Nd: YAG laser beam verses incident beam power spatial density

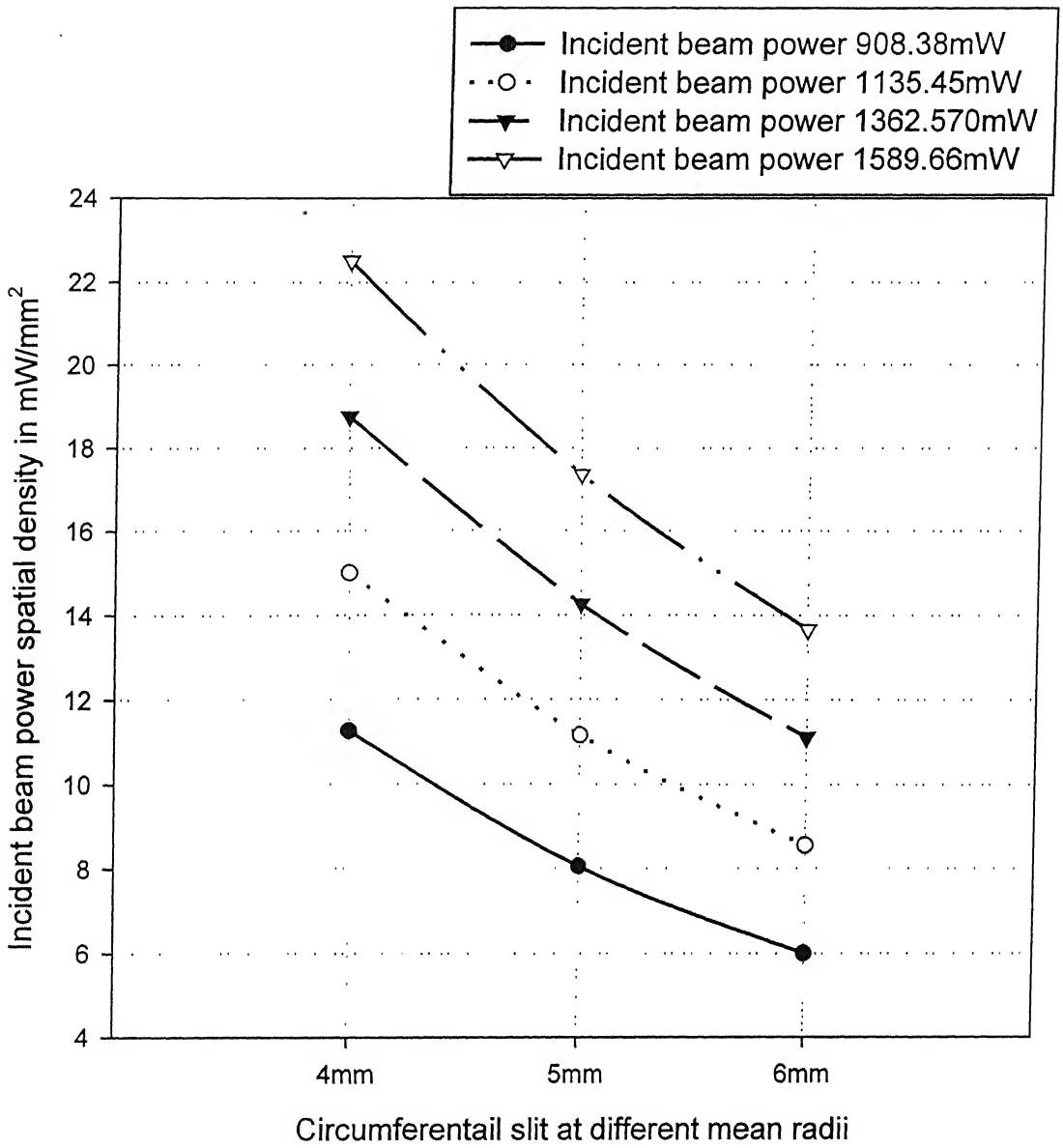


Fig. 5.8 (d) Comparison of incident beam power spatial density with increased mean radii

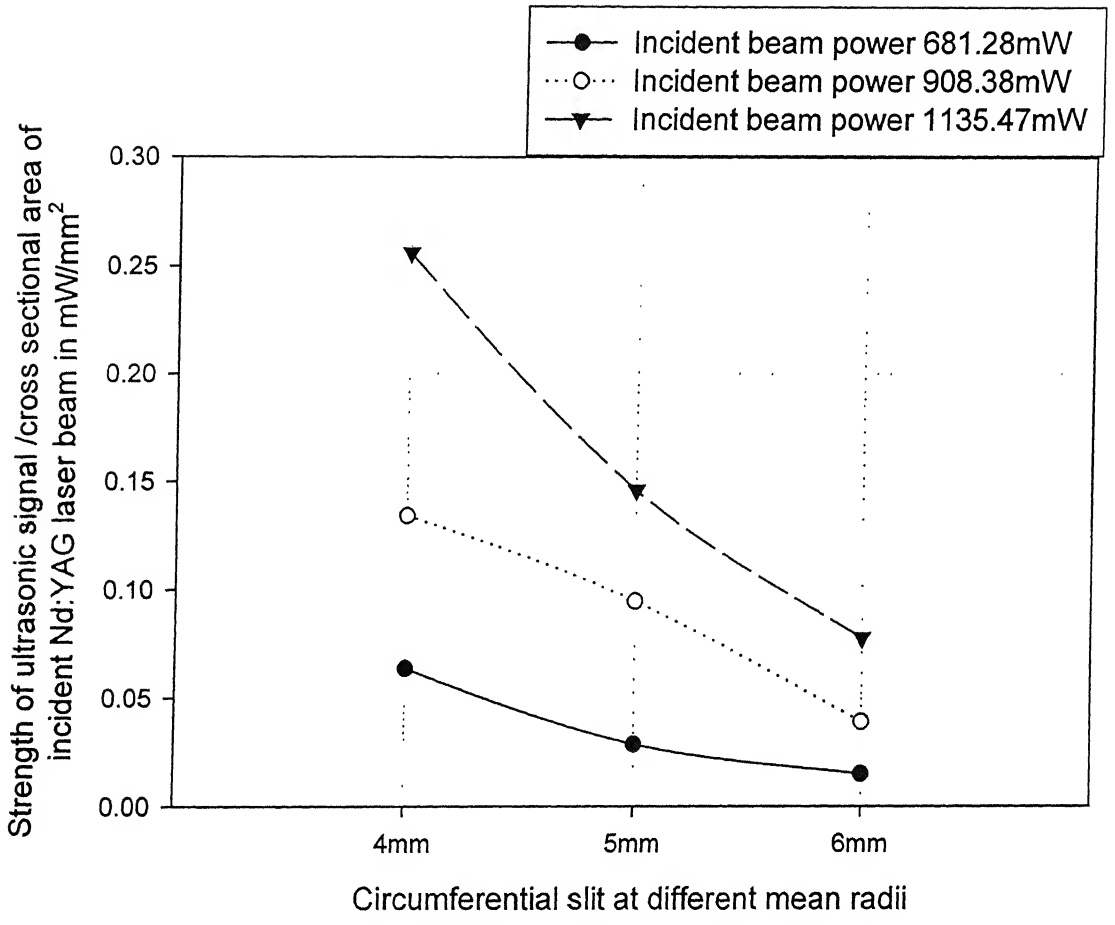


Fig. 5.8 (e) Comparison of ultrasonic signal strength/ cross sectional area of incident Nd: YAG laser beam with increased mean radii (material: aluminium)

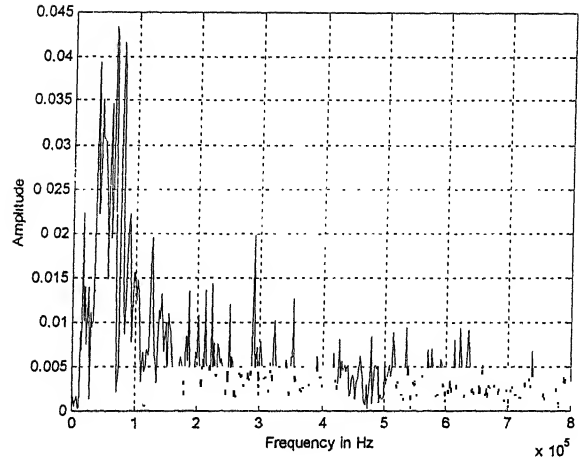


(a) Specimen before focal length

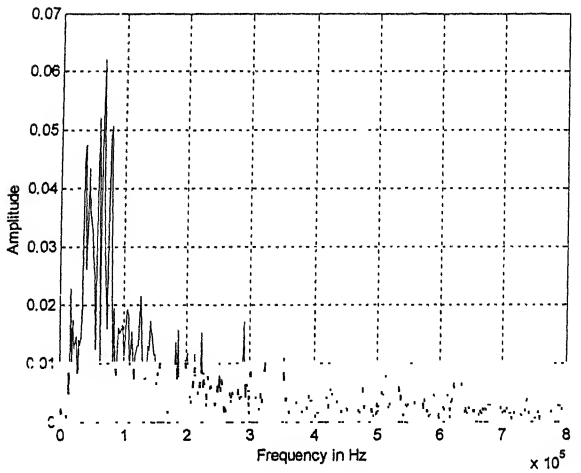


(b) Specimen at focal length

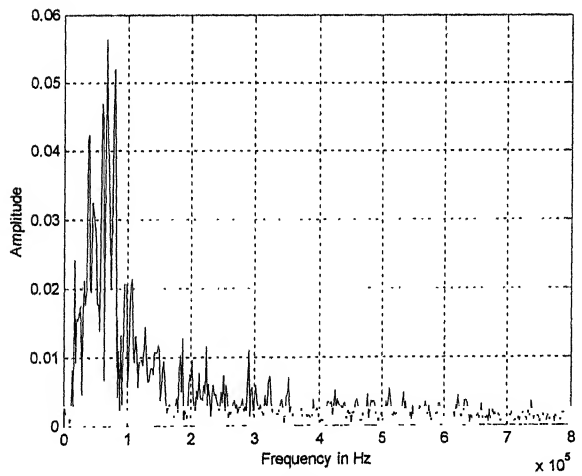


(c) Specimen after focal length

Fig.5.9 Amplitude spectrum at incident beam power at 2270mW (material: aluminium)

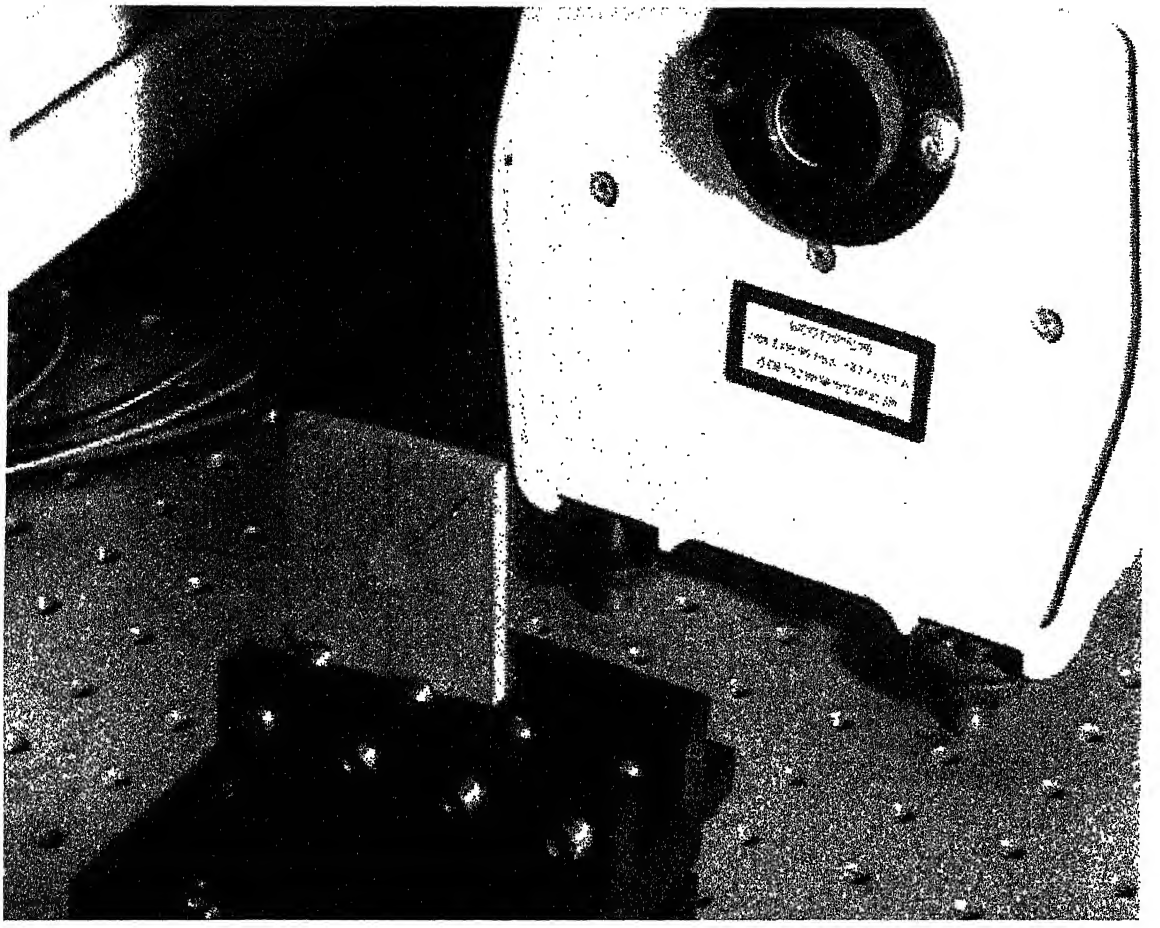

Fig.5.10 Photograph of the ablated specimen (Aluminium)

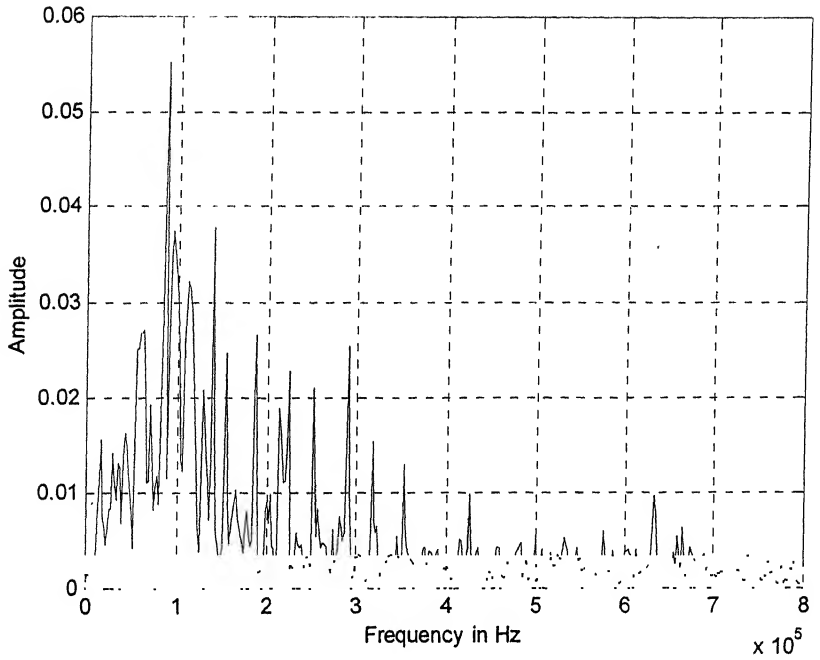


Fig. 5.11 Amplitude spectrum at incident beam power of 2725mW (material: aluminium)

*Chapter 6*

# CONCLUSIONS AND SCOPE FOR FUTURE WORK

In the present work, an experimental technique has been developed using an Nd: YAG pulsed laser for generation of ultrasonic waves in specimens and a He-Ne continuous laser based heterodyne optical interferometric probe for detection of the same. Based on the results obtained, the following conclusions are drawn:

## 6.1 CONCLUSIONS

1) The Nd: YAG laser beam is of 7mm diameter and very intense at the center and decreases towards the periphery.
2) The power distribution within the beam is Gaussian in nature.
3) The generated ultrasonic signal depends upon the specimen material. The ultrasonic wave is of predominantly single frequency in nature (79.87 kHz for aluminium and 119.8 kHz for glass-epoxy composites) if Nd: YAG laser is of low power as possibly it is in thermoelastic regime; while the ultrasonic wave is of broad band if the power input is of high value possibly it being in ablation regime.

## 6.2 SCOPE FOR FUTURE WORK

1) Reduction of scanning noise and fluctuations in energy levels of ultrasonic source laser can be reduced by
    a. Exploring the possibility of applying paint, oil to irradiated surface as this may improve the ultrasonic characteristics. This will also make it possible to use higher power settings without worrying about ablating the composite specimen.
    b. A peelable retroreflective film has been identified for adhering onto surface interrogated by the heterodyne interferometer. This gives an

approximately uniform response (<3 dB variation) over a scan on a relatively smooth surface.

2) More experimental work on ultrasonic data collection of several material systems is necessary for good conclusive statements.

# *References*


[1] "History of lasers", Downloaded from http://www.columbia.edu/cu/mechanical/mrl/ntm/level1/ch02/html/l1c02s03.html

[2] Sirohi R.S."A course of experiments with He-Ne Laser", Wiley Eastern Limited, Second edition, May 1991.

[3] Keicher, David M. " Laser beam Characterization results for a high-power cw Nd: YAG laser", Proceedings of SPIE- The international Society for Optical Engineering, Vol 2375, 1995, pp.162-171.

[4] Scruby and Drain. "Laser Ultrasonics Techniques and Applications", Adam Hilger Bristol, Philadelphia and New York, 1990

[5] Monchalin J.B., "Optical Detection of Ultrasound", IEEE Transactions on Ultrasonics, Ferroelectrics, and Frequency control, Vol UFFC-33, no. 5 September 1986, pp. 485-499

[6] Huber R.D. and Green R.E., Jr., " Noncontact Acousto-Ultrasonics Using Laser Generation and Laser Interferometric Detection", Materials Evaluation May 1991, pp.613-618.

[7] Christine Corbel, Franck Guillois, Daniel Royer, Mathias A. Fink, and Rene DE Mol, "Laser-Generated Elastic Waves in carbon-Epoxy Composite", IEEE Transactions on Ultrasonics, Ferroelectrics, and Frequency Control, Vol 40, No. 6, November1993, pp. 710-716

[8] Castagnede B., Marc Deschamps, Eric Mottay and Andre Mourad, " Laser impact generation of ultrasound in composite materials", Acta Acustica 2 (April 1994), pp. 83-93.

[9] Hideo Cho, Shingo Ogawa and Mikio Takemoto, "Non Contact laser ultrasonics for detecting subsurface lateral defects", NDT&E International, Vol 29, No.5, pp.301-306, 1996.

[10] S.K. Rathore, N.N. Kishore, P. Munshi and W. Arnold, "Defect Location and Sizing Using Laser Based Ultrasonics (LBU)", Submitted for publication.

[11] Legendre S., Goyette J., and Massicotte D. "Ultrasonic NDE of composite material structures using wavelet coefficients", NDT&E International, Vol. 34, No. 1, January 2001, pp. 31-37.

[12] Krautkramer Josef, Krautkramer Herbert. "Ultrasonic Testing of Materials", Springer-Verlag Berlin Heidelberg, New York, 1983.

[13] Oppenheim Alan V., Willsky Alan S. "Signals & Systems", Eastern Economy Edition, Prentice-hall India, 1997.

[14] Cerini Michael and Harvey Audrey F. "The Fundamentals of FFT-Based Signal Analysis and Measurement", Downloaded from http://www.ni.com/

[15] Sarin, P.S. "Development of laser based ultrasonics non-destructive testing", M.Tech. Thesis, January 2002, Department of Aerospace Engineering, Indian Institute of Technology, Kanpur.

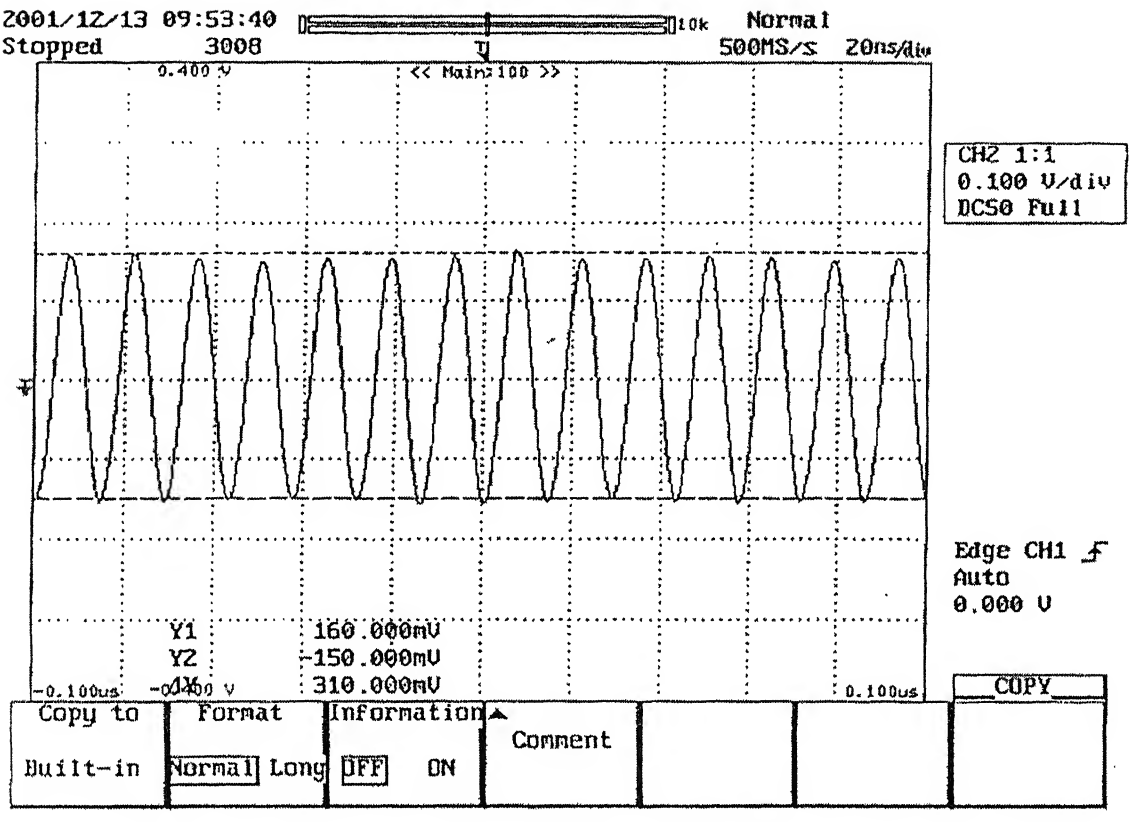


**Photo Detector Output Measured Without Going Through The Signal Processor.**

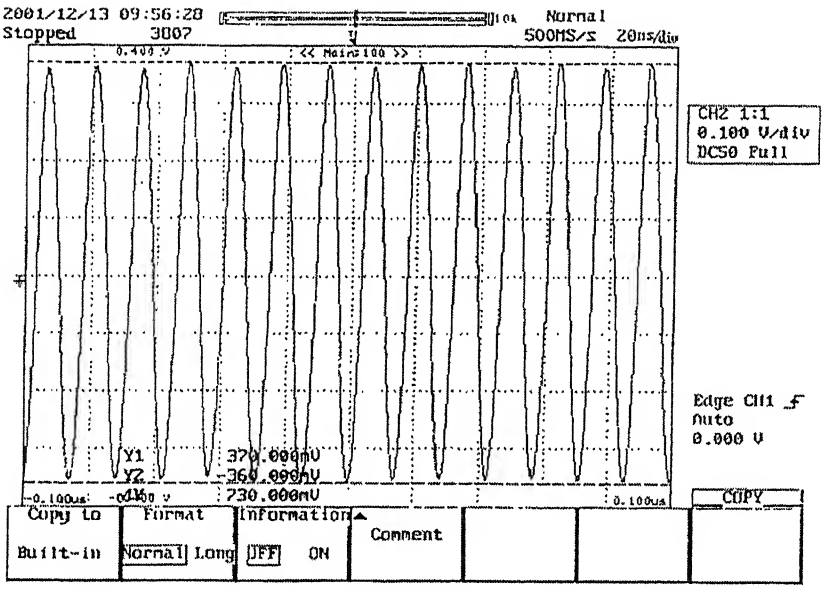


**Output Taken Through The Signal Processor With The Automatic Gain Control Switched On.**

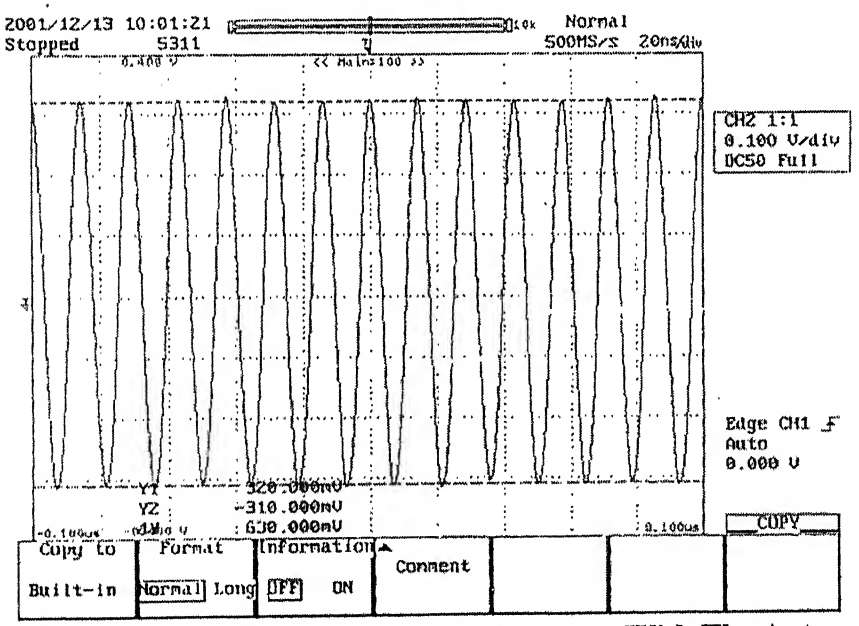


**Output Taken Through The Signal Processor With The Automatic Gain Control Switched On After Making Adjustments Available In The Signal-Processing Unit In order To Set It To 630mv.**

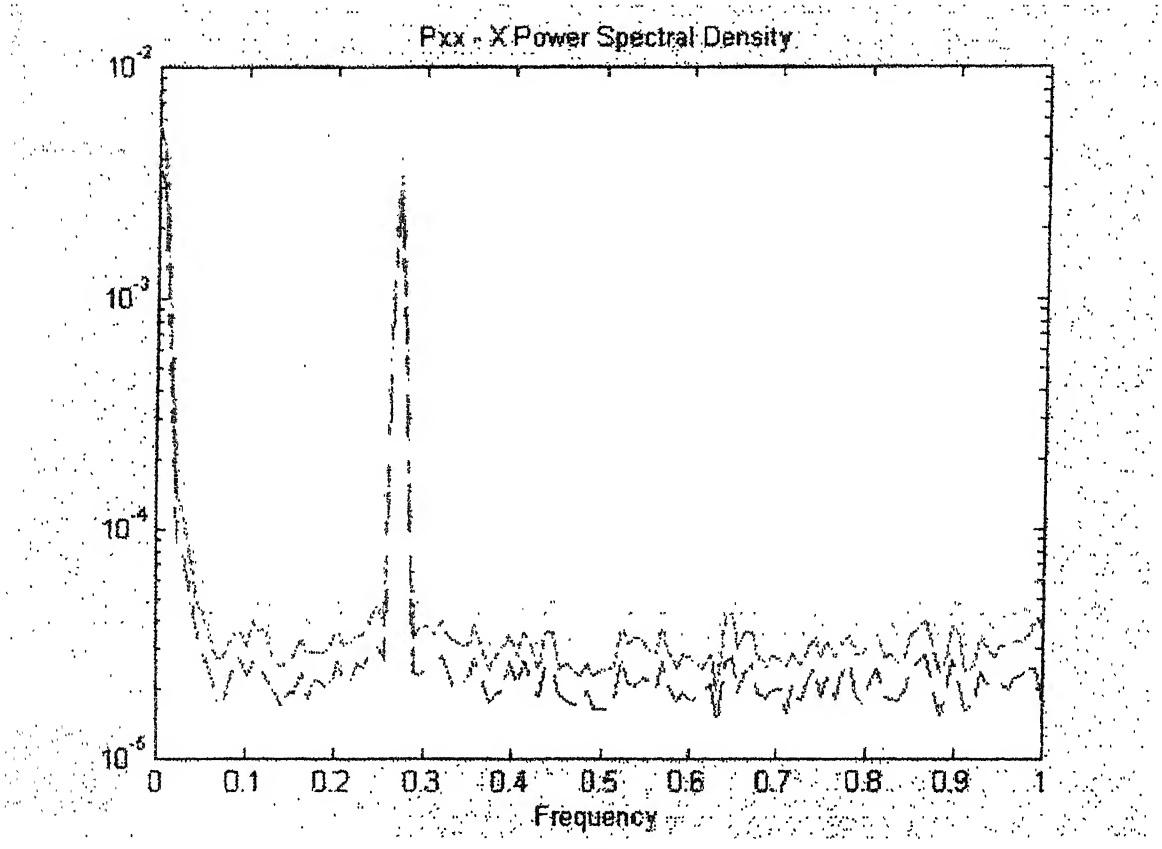


**Power Spectrum Display In Matlab Used To Measure Sensitivity Of Heterodyne Interferometer. (The Measured Sensitivity Was 10 Mv/ A°.)**

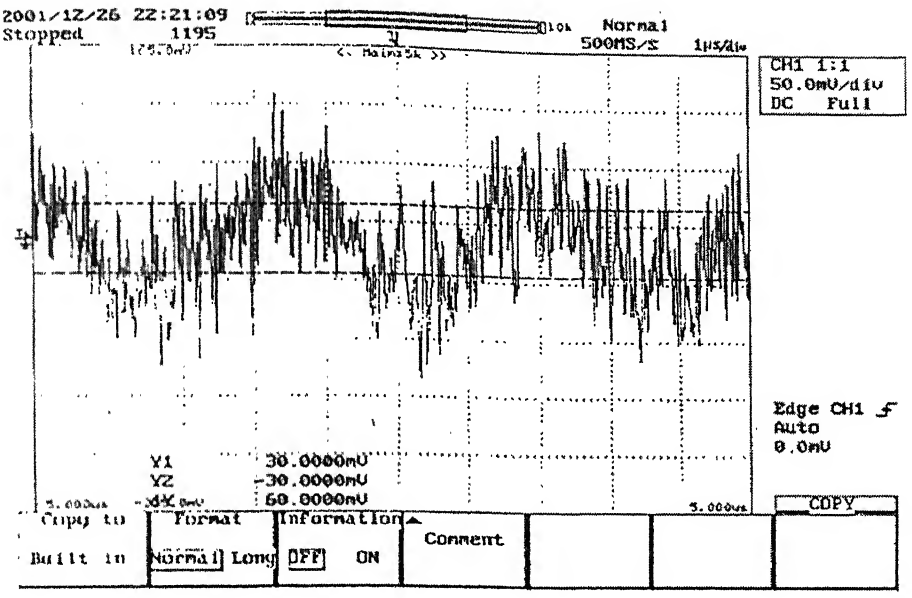


**Detectivity Measurement (18MHz Bandwidth) Displacement 3A°**

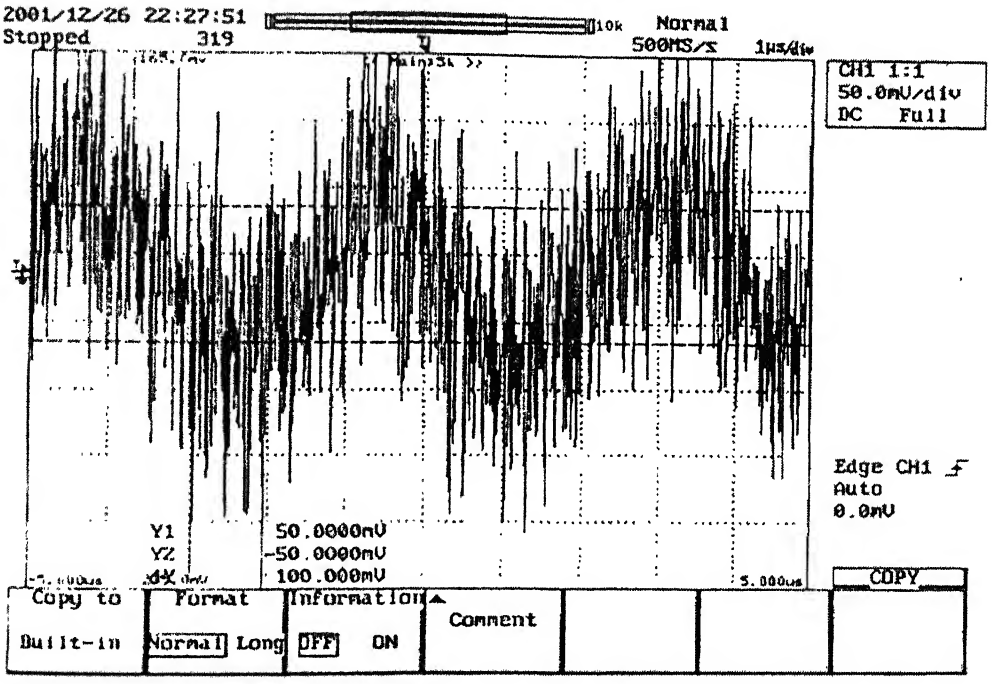


**Detectivity Measurement (45MHz Bandwidth) Displacement 5A°**

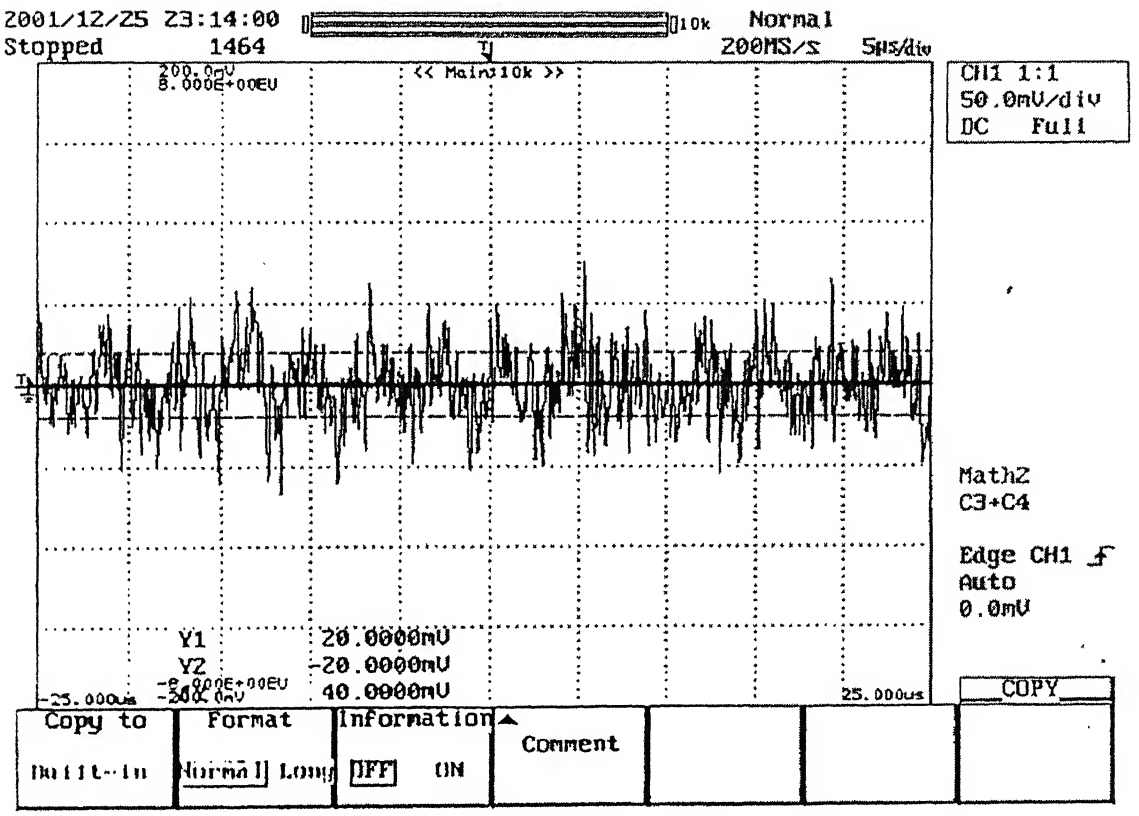


**Detectivity Measurement (4MHz Bandwidth) Displacement 2A°**

**%Matlab Program for plotting the Amplitude versus frequency plots**

```
k=input('Enter the no.of passes');
n=zeros(10020,7);
ff=zeros(10020,7);
freq=zeros(10020,7);
l=zeros(10020,7);
g=zeros(10020,7);
h=zeros(7);
for j=1:k

FID=fopen(input('Enter the file name\n','s'));
aa= fscanf(FID,'%e',10020);
g(:,j)=g(:,j)+aa;

end
for j=1:k

n(:,j)=n(:,j)+fft(g(:,j),10020);
ff(:,j)=ff(:,j)+abs(n(:,j))/10020;
freq(:,j)=freq(:,j)+(2e4*(0:10019))';
hh(j)=h(j)+sum(ff(:,j))/10020;
l(:,j)=l(:,j)+j*ones(10020,1);

end
hh
ff(1,:)=zeros;
ff=ff(1:256,:);
freq=freq(1:256,:);
l=l(1:256,:);
plot3(l,freq,ff,'b')
title('Plot fof aluminium material');
ylabel('Frequency in Hertz');
xlabel('1mm dia.hole at various positions');
zlabel('Amplitude');
axis([-inf inf -inf inf –inf inf])
grid on
hold on
rotate3d on
```

**%Matlab Program for calculating power of signals**

```
k=input('Enter the no.of passes');
p=input('Enter the no.of power settings');
E=zeros(p,k);
bb=zeros(10020,7,7);
n=zeros(10020,7,7);
ff=zeros(10020,7,7);
gg=zeros(10020,7,7);
hh=zeros(p,k);
kk=zeros(p,k);

for j=1:p
for i=1:k


FID=fopen(input('Enter the file name\n','s'));
aa= fscanf(FID,'%e',10020);
bb(:,j,i)=bb(:,j,i)+aa;
kk(j,i)=kk(j,i)+sum(bb(:,j,i).*bb(:,j,i));
n(:,j,i)=n(:,j,i)+fft(bb(:,j,i),10020);

ff(:,j,i)=ff(:,j,i)+(n(:,j,i).*conj(n(:,j,i)))/10020;
hh(j,i)=hh(j,i)+sum(ff(:,j,i));
E(j,i)=E(j,i)+hh(j,i);
end
end
power=E/10020;
```